Structural controls on the Bonsucesso Zinc-Lead Deposit, Vazante Group, Brazil

Edson Ricardo Maia Ferraz[1]* ⓘ, George Luiz Luvizotto[1] ⓘ, Juliana Okubo[2] ⓘ, Denis Antonio Batiston[2] ⓘ

Abstract

The Bonsucesso zinc-lead (Zn-Pb) sulfide deposit is hosted in carbonate rocks from the Vazante Group (transition of the Mesoproterozoic to the Neoproterozoic time), northwest of Minas Gerais State, Brazil. Regional deformation is associated with the thin-skinned tectonics that led to the formation of the foreland zone of the Brasília Orogen during the Neoproterozoic. These orogenic processes are the trigger of Zn-Pb mineralization in many base-metal deposits in the Vazante Group. Here, we describe the ore textures and the structures of the deposit to define its structural controls in deposit scale and formulate hypotheses about its forming process in the context of other Vazante Zn-Pb deposits. Mineralization distribution is controlled by a high-angle fault zone striking NNW and dipping 60° to WSW. Fault-related fractures functioned as pathways for Zn-Pb-rich fluids to be redistributed and crystallize where chemical conditions were adequate. Mineralization was likely formed in an extensional setting in breccia zones controlled by flexurally induced normal faults related to development of the foreland basin of Brasília Orogen. Later, the entire Vazante sequence underwent an inversion process and extensional structures were reactivated or obliterated. Finally, an understanding of local controls may be of good use to target exploration for new orebodies in the district scale.

KEYWORDS: zinc; structural geology; MVT; Brasília Belt; Morro do Calcário Formation.

INTRODUCTION

Geological structures play a fundamental role in almost all types of mineral deposits. Thus, a better understanding of the structural architecture of the mineralization is a powerful guide to grade continuity and may reduce misinterpretations (Cowan 2014). The relevance of fault systems as host structures for hydrothermal mineralization has long been reported in many deposit types, such as sediment hosted Pb-Zn-Ag, lode Au, and iron oxide Cu-Au deposits (Newhouse 1942, McKinstry 1948, Sibson 1996, Cox 2005). Furthermore, the formation of fault-fracture networks and fluids redistribution in extensional and transtensional regimes plays a crucial role in the formation of many hydrothermal mineral deposits (Sibson 1996, 2000). On the contrary, base-metal deposits related to contractional faults have also been reported, and infilling of mineralization fracture–meshes coeval with compressive settings has been recognized (Ghazban et al. 1994, Liaghat et al. 2000, Hou and Zhang 2015, Zhang et al. 2017).

The Bonsucesso zinc-lead (Zn-Pb) sulfide deposit hosted in carbonate rocks of Morro do Calcário Formation, Vazante Group was recently discovered in the Paracatu region, northwestern Minas Gerais. Although the Vazante Group age is still a matter of debate, there is a general agreement that the upper section of this sedimentary sequence was deposited at about 1000 Ma in the transition of the Mesoproterozoic to the Neoproterozoic (Dardenne 2000, Misi et al. 2014). Together with the known deposits of Vazante (total estimated resources of 60 Mt at 20% Zn), Morro Agudo (total estimated resources of 20 Mt at 5.0% Zn and 1.75% Pb), Ambrósia Sul (2.15 Mt at 5.0% Zn and 0.16% Pb), and Fagundes (2.8 Mt at 4.0% and 0.3% Pb), this discovery is a part of the best-endowed district for Zn of Brazil (Fig. 1A).

At the Bonsucesso deposit, major faults are related to the Brasiliano orogeny (ca 900 Ma–600 Ma, Pimentel 2016), the last tectonic event that led to development of the Brasília fold-thrust belt and affected the Vazante Group (Almeida et al. 1981, Dardenne 2000, Valeriano et al. 2004, 2008).

The aim of this paper is to characterize the structural controls, ore textures, and geometry of the Bonsucesso Zn-Pb sulfide deposit and to understand its formation. Our study is based on the integration of drill core data, structural analysis of oriented-drill cores, 3D geological modeling, and petrography. Here, we describe the structures, ore, and gangue minerals, discuss its relationships in the deposit and regional scale, and try to formulate hypotheses about its forming processes. Our work might offer contributions to the understanding of local controls of mineralization, and it may be of good use to target exploration for new orebodies in the district scale.

[1]Universidade Estadual Paulista "Júlio de Mesquita Filho", Institute of Geosciences and Exact Sciences, Department of Petrology and Metallogenesis – Rio Claro (SP), Brazil. E-mails: erm.ferraz@unesp.br, george.luvizotto@unesp.br, dabatiston@gmail.com

[2]Universidade Estadual Paulista "Júlio de Mesquita Filho", Institute of Geosciences and Exact Sciences, Department of Applied Geology – Rio Claro (SP), Brazil. E-mail: julianaokubo@yahoo.com.br
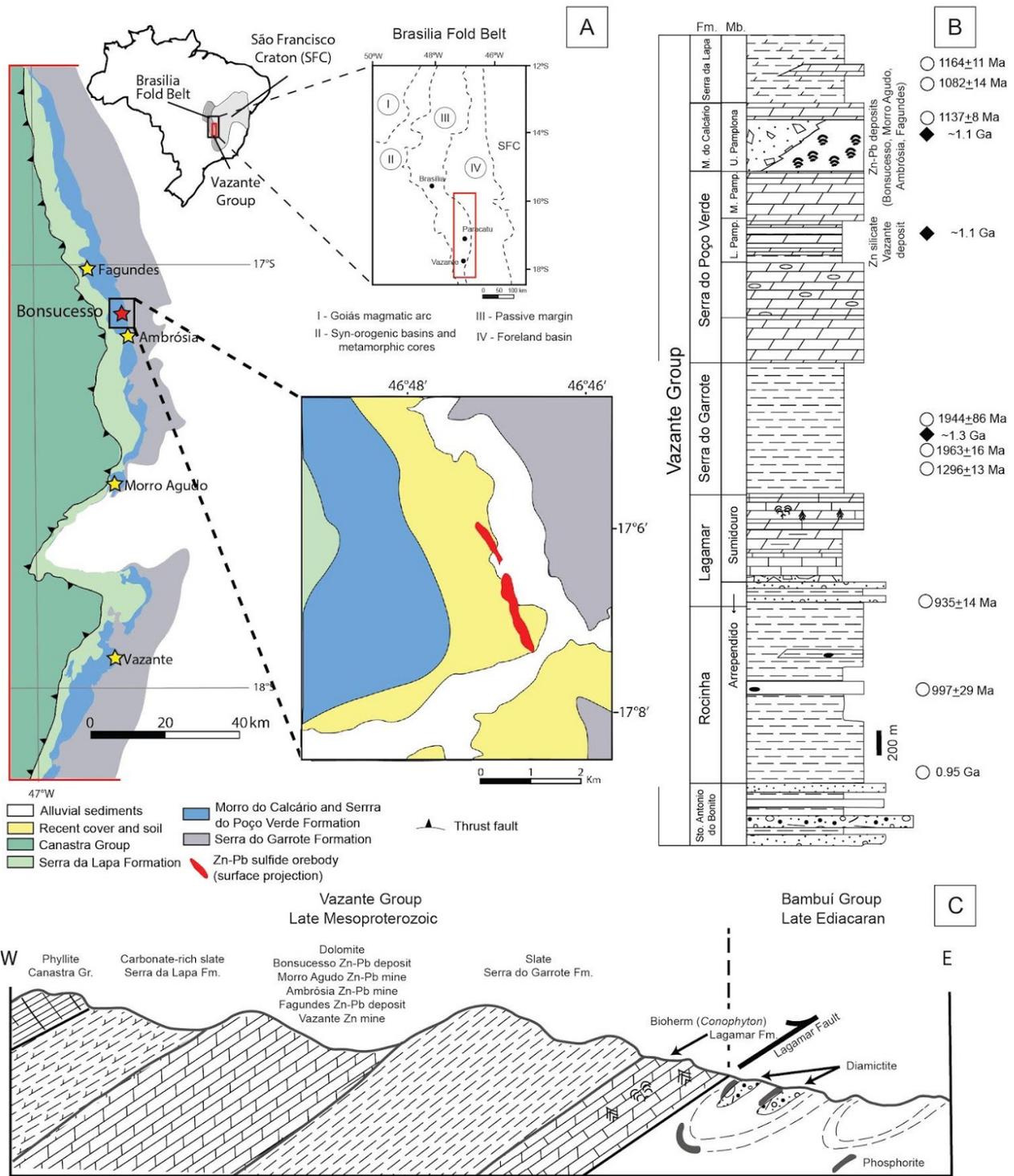
*Corresponding author.

Figure 1. Location of the Bonsucesso Zn-Pb sulfide deposit. (A) Simplified geological map of Vazante Group (former passive margin of São Francisco paleoplate) at eastern portion of the Brasília Belt. Red star represents the Bonsucesso deposit and yellow stars represent the other Zn-Pb deposits in the area. Zoomed-in box shows the projection of Zn-Pb mineralization zone over soil and recent sediments. (B) Schematic lithostratigraphic column of the Vazante Group (after Dardenne 2001) and the stratigraphic position of its Zn-Pb deposits. At right, geochronological data: White circles are U-Pb detrital zircon ages from Rodrigues *et al.* (2012); Black diamonds are Re-Os ages from Azmy *et al.* (2008) and Geboy *et al.* (2013). (C) Schematic geological cross section at the southern sector of Vazante Group (modified from Misi *et al.* 2014). Lagamar thrust fault juxtaposed older sediments of Vazante Group and younger sediments of Bambuí Group.

REGIONAL GEOLOGY AND STRUCTURAL FRAMEWORK: A REVIEW

The Bonsucesso deposit is located in the Paracatu region, northwest of Minas Gerais State, Central Brazil. Zn-Pb sulfide mineralization is hosted in rocks of the Vazante Group, (Tonian period, ca 1000 Ma, Carvalho *et al.* 2019, Dardenne 2000, Misi *et al.* 2014) on the southeast sector of Brasília Belt.

The origin of this fold-and-thrust belt dates back to the São Francisco paleoplate late Mesoproterozoic to early

Neoproterozoic rifting to full passive margin development (Almeida 1967, Almeida *et al.* 2000, Pimentel *et al.* 2001, Catuneanu *et al.* 2005, Martins-Neto 2009) and it ends as the São Francisco paleoplate subducted to the west during the assembly of West Gondwana (Dardenne 2000, Romeiro-Silva and Zálan 2007, Martins-Neto 2009).

The understanding of the Brasília Belt evolution (Almeida 1967, Pimentel and Fuck 1992, Dardenne 2000, Valeriano *et al.* 2008, Sial *et al.* 2009) has increased over the years and new geochronological and isotopic data have helped to better constrain major tectonic compartments (for recent reviews see Pimentel *et al.* 2011, Cordani et al. 2013a, 2013b, Araujo *et al.* 2014, Brito Neves and Fuck 2014, Brito Neves *et al.* 2014, Pimentel 2016, Carvalho *et al.* 2019). From west to east, the Brasília Belt can be subdivided as shown in Fig. 1A: Goiás magmatic arc, syn-orogenic basins and metamorphic core, passive margin (the supracrustal sequences of the fold-and-thrust belt primarily deposited over the São Francisco craton margin), and foreland basin (cratonic cover) (Pimentel *et al.* 2011, Pimentel 2016).

The Vazante Group (Dardenne *et al.* 1998, Dardenne 2000) extends N-S through nearly 250 km in length, with an average width of 30 km (Fig. 1A). To the west, it is bounded by the Canastra Group (similar age), and to the east, by the Bambuí Group. Metamorphic conditions reached peak at low greenschist facies (Monteiro *et al.* 2006) with development of pervasive axial plane cleavage in general parallel to bedding and formation of crenulation cleavage related to isoclinal folding and later open folds, respectively (Carvalho *et al.* 2016).

This unit constitutes a thick metasedimentary sequence originally deposited in shallow waters of the São Francisco paleoplate passive margin. It is divided into seven formations (Fig. 1B), from base to top: Santo Antônio do Bonito, Rocinha, Lagamar, Serra do Garrote, Serra do Poço Verde, Morro do Calcário, and Serra da Lapa (Dardenne *et al.* 1998, Dardenne 2000). The basal Santo Antônio do Bonito and Rocinha formations are composed of metapelitic units with phosphate concentrations (Dardenne 2000).

According to Dardenne *et al.* (1998) and Dardenne (2000), the Lagamar Formation represents a metapsamo-pelitic unit with basal metaconglomerates, dolomitic breccia, dark gray limestone, and stromatolitic bioherm with columnar stromatolites of the *Conophyton* and *Jacutophyton* types. The Serra do Garrote Formation represents a sequence of pyrite (Py)-bearing carbonaceous gray slate and quartzite layers. The Serra do Poço Verde Formation is made up of gray to pink algal-laminated dolomite, gray to green slates, sericite phyllite, dark gray dolomite with bird's-eyes, marls, and Py-bearing carbonaceous shale. The Morro do Calcário Formation is composed of stromatolitic bioherm facies, intraformational breccia, dolarenite, and subordinate carbonaceous shale. These two formations correspond to the dominantly dolomitic sequences that host the Zn–Pb deposits and can represent a continuously deposited dolomitic sequence. The dolomitic sequence is overlain by the Lapa Formation, with

black rhythmic carbonaceous slate and phyllite (Serra do Velosinho Member) and sericite–chlorite phyllite, carbonate-bearing metasiltstone, dolomite, and quartzite lenses (Serra da Lapa member).

The area has been studied since the 1950s, but the Vazante Group age is still an unresolved problem, mainly due to the absence of absolute markers (e.g., volcanic ash layer) and the wide span in time provided by the fossil record (*Conophyton* stromatolite, 1.35 Ga–0.95 Ga).

An Rb-Sr whole rock isochron for shales from Vazante Group yielded an age of 600 + 50 Ma (Amaral and Kawashita 1967), which could represent the last closing of the isotopic systems during the Brasiliano metamorphic event. Re-Os ages in organic-rich slates of the Vazante Group (Azmy *et al.* 2008, Geboy *et al.* 2013), and U-Pb ages of detrital zircons in quartzites distributed along the whole sequence (Rodrigues *et al.* 2012) provided a late Mesoproterozoic age for the top and an early Neoproterozoic age for the basal units. Furthermore, these late Mesoproterozoic ages agree with seismic, well, and outcrop data that correlate the Vazante Group with the Macaúbas Group located on the east side of São Francisco craton. Both units comprise first-order sedimentary sequences developed over the São Francisco craton margins when supercontinent Rodinia broke up (Martins-Neto 2009, Alkmim and Martins-Neto 2012). Based on the geochronological data and field relations, Misi *et al.* (2014) argued that the upper and older section (Lagamar to Serra da Lapa formations) was thrusted (Lagamar fault zone) over the younger lower section (Santo Antonio do Bonito and Rocinha formations). Misi *et al.* (2014) also suggested a correlation between part of the Vazante Group lower section and the Serra da Saudade Formation of the Bambuí Group (Fig. 1C).

Currently, the biggest base-metal deposits of Vazante Belt are Morro Agudo (Zn-Pb sulfide deposit with 20 Mt at 5.0% Zn and 1.75% Pb) and Vazante (world's largest hypogene non-sulfide Zn deposit with 60 Mt at 20% Zn, including willemite-ore and supergenic-ore). Vazante Group deposits are hosted in carbonate rocks close to the margin of an uplifted foreland basin and their Zn-Pb ore-minerals contain saline fluid inclusions, both features suggest genetic similarities to Mississippi Valley-type deposits (Appold and Monteiro 2009). These deposits, hosted in carbonate-dominated sequences, formed from basinal brines expelled as a result of tectonic activity (Leach *et al.* 2010). However, the hypogene Zn silicate of Vazante deposit differs significantly from this model regarding the ore-type and homogenization temperature (Monteiro *et al.* 1999, Appold and Monteiro 2009).

Structural framework

The sedimentary rocks of the Vazante Group, originally deposited along the margin of the São Francisco-Congo paleoplate, were affected by thin-skinned tectonics as São Francisco-Congo paleoplate subducted underneath the Brasília orogen. Seismic lines from Romeiro-Silva and Zálan (2007) clearly exhibit a deformation of shallow

allochthonous thrust sheets of the Vazante, Canastra, and Bambuí groups.

At the seismic sections's western edge, the sheets are shortened and lie over the décollement zone, which marks the unconformity that separates them from the Paranoá/Macaúbas megasequence.

Based mainly on reflection seismic, the advancing knowledge of the São Francisco craton and its surrounding fold-and-thrust belts has allowed for better stratigraphic correlations between Proterozoic sedimentary megasequences and to devise robust structural frameworks (Alkmim and Martins-Neto 2012, Romeiro-Silva and Zálan 2007).

Despite its economic relevance, the northern Vazante Group was addressed only by a few studies concerning its structural geology, and most of these studies were carried out in the southern sector of this unit (Campos Neto 1984, Pinho *et al.* 1989, Pinho 1990, Freitas-Silva 1991, Pereira 1994, Rostirolla 2002, Marcia 2014). The east movement direction of thrust sheets is inferred by sinuous and mostly convex fault traces on the map. Mineral and stretching lineations indicate the same direction of movement. An interesting aspect of the map trace is the Rio Escuro reentrant. This syntaxial curve (concave toward the foreland) basically divides the belt into two sectors (north and south). The arcuate structure may be a result of the differential advance of the thrust front over a basement high. Rio Escuro reentrant forms a topographic low covered by recent sediments. Coincidently or not, the reentrant marks profound stratigraphic changes (the lack of Serra do Poço Verde formation to the north of it) and peculiar conditions of ore-forming fluids (occurrence of Zn-silicate ore only to the south of it). Zn-Pb deposits (e.g., Morro Agudo and Vazante mines) are at the maximum advance of the thrust front, where the sedimentary pile is thicker.

One major compressive and progressive deformation event is well recognized in the Vazante Group and was responsible for the formation of the slaty cleavage (S0/S1) and isoclinal folding. Strike-slip faults related to the progression of this event are also documented, besides late folds that affected the previous planar structures. Finally, an extensional phase postdating the compressive structures is also reported (Campos Neto 1984, Pinho 1990, Freitas-Silva 1991, Pereira 1994, Rostirolla 2002, Marcia 2014, Carvalho *et al.* 2016). Folds and thrusts developed during the thin-skinned tectonics in the Vazante Group have east vergence direction. Thrust faults are low-angle and dip west at 30°–35°. There are high-angle reverse faults that probably formed because of folding, ancient normal fault reactivations, and fault rotation.

METHODS

A thick soil layer (approximately 30 m) occurs on top of the Bonsucesso deposit, and no rocks crop out in the studied area. Since detailed field mapping is not possible, the work was carried out using drill hole data and the 3D geological modeling software Leapfrog Geo®.

An electron microprobe JEOL, model JXA-8230, equipped with 5 WDS detectors, EDS detector type SSD, secondary electron detectors, and backscattered electrons (BSE), was used to acquire the compositional maps for carbon (C), Cd, silica (Si), Fe, Mn, and Zn (accelerating voltage of 15 kV and probe current of 100 nA). EPMA maps results were processed using the XMapTools software (Lanari *et al.* 2014, 2019).

Structural measurements were collected from oriented drill cores according to the following procedures. Inclined drill holes were oriented using the core stub technique, i.e., a steel spear with a sharp point was lowered inside the rods to mark the position of the gravity vector (i.e., to determine the bottom of the hole) on the core stub after the extraction of a full core barrel (Zimmer 1963, Marjoribanks 2010). However, most of the drill holes were oriented using the core barrel method, which orients the drill hole at the moment when the lowest piece of the core is gripped by the lifter before breaking it free (Marjoribanks 2010). The electronic device used was the Reflex ACT III. After the extraction of the core barrel, bottom (or top) of hole marks were made. Thus, broken drill core pieces were laid out over a channel to be reassembled as much as possible. After the reassembling, bottom lines were traced along the run with arrows pointing down-hole.

Three techniques were applied to measure structures:

i.   the rocket launcher, which consisted of a wood set that replicates drill rig orientation at the coreshed and allows geologists to position oriented core samples as they were in situ and so collect structures;

ii. the measurement of internal core angles (alpha, beta, and gamma) later transformed by the Leapfrog Geo® software or spreadsheet into the real strike and dip or trend and plunge values already corrected by the desurveying methods;

iii. the vSET™ method, another technique also based on geometrical relationships and more suitable to the measurement of linear structures.

GEOLOGY OF THE BONSUCESSO DEPOSIT

Lithology and stratigraphy

Two lithostratigraphic units from the Vazante Group occur at Bonsucesso deposit: Serra do Garrote Formation and Morro do Calcário Formation. The hydrothermal dolomitic breccia containing the Bonsucesso orebodies is hosted in metapelite and carbonate rocks of the Morro do Calcário Formation (Fig. 2). Rocks of Serra do Garrote Formation were emplaced within the Morro do Calcário unit by a reverse fault. The following lithological description is restricted to hanging wall and footwall rocks of the Bonsucesso fault-controlled deposit.

Soil

The Bonsucesso deposit lies under a 30-m-thick deposit composed of allochthonous soil and recent sediment.
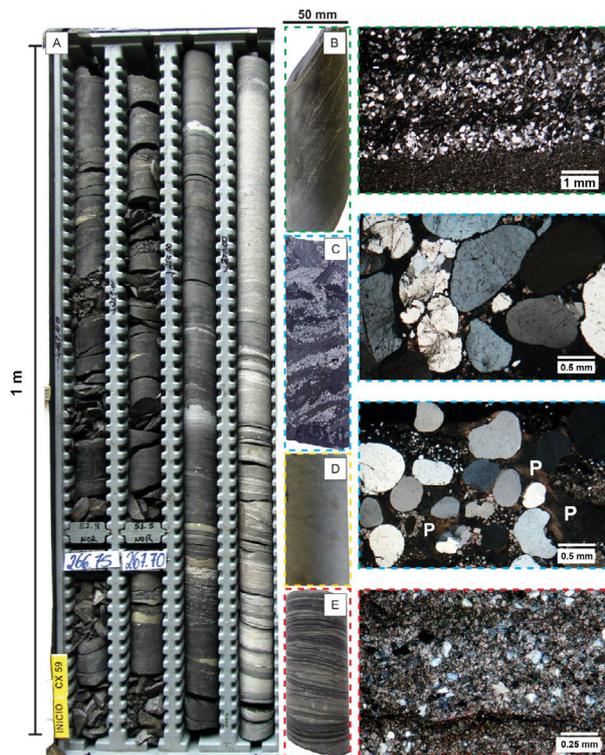
Figure 2. Lithotypes and rock textures of the Bonsucesso deposit. (A) Transition of metamarl (carbonate mudstone) to black carbonaceous phyllite. These rocks occur interbedded within the Morro do Calcário Formation. (B) Carbonaceous phyllite with bedding marked by quartz-rich layers and carbonaceous mica-rich layers (Serra do Garrote Formation). Cross polarized light. (C) The core sample exhibits a mixture of coarse clasts of carbonate rocks and well-rounded quartz sand in a fine black matrix. A photomicrograph shows a heterogeneous origin for quartz sand, including lithic clasts and quartz with wavy extinction. Microcrystalline phosphate (P) also occurs in the matrix as cement. (D) Fine dolostone with discrete bedding. (E) Metamarl (carbonate metamudstone). Bedding is marked by alternating mm- to cm-thick carbonate-rich layers and mica-rich layers. Note on the thin section (photomicrograph) the presence of clasts of muscovite and quartz. Cross polarized light. See Fig. 3 for the location of these lithotypes.

The soil cover has a distinctive 5-m-thick clay-rich layer enriched in magnetite, which consists of red and orange clay and quartz-rich material mixed with clasts of dolostone and chert (Araujo 2019). This soil coverage acts as a barrier (no compelling geochemical anomaly occurs on the surface over the mineralized zone) and conventional geochemical and geophysical techniques are not efficient tools for mineral exploration.

Serra do Garrote Formation

The Serra do Garrote Formation consists of black to gray carbonaceous phyllite (Fig. 2B). Occurrences of 1–3-cm-radial Py nodules and also fine layers of Py parallel to bedding are common. Near the fault zone, these rocks are brecciated and veining by calcite and quartz is strong.

Morro do Calcário Formation

A variety of rocks comprise the hanging wall and footwall blocks. Massive micritic dolostone, columnar stromatolitic dolostone, dolorudite with lamellar breccia, dolarenite, intraformational breccia, oolitic dolostone, and laminated dolostone (Fig. 2D) are the main lithotypes. Void-filling white dolomite occurs as veins near the damage zone and fault core. Dark chert veins are also related to hydrothermally altered zones. Below the soil cover, weak acidic water flow has promoted strong dissolution of dolostone along bedding planes, joints, fractures, and fault zones to form an intricate system of caves at shallower levels.

Within the dolomite unit, there is a distinctive package of carbonate metamudstone (also referred as metamarl) whose thickness varies from 80 m in the south sector and gradually decreases to 40 m in the north sector. These rocks are interbedded thin carbonaceous mica-rich layers and micritic dolomite with minor terrigenous contribution (clasts of quartz and feldspar) that occur in the hanging wall and footwall blocks (Figs. 2A and 2E). Within this carbonate metamudstone layer, a 1–2 m-thick bed of a mixture of siliciclastic and carbonate material occurs (Fig. 2C). The carbonate layers are composed of fine angular clasts in matrix and gravels of dolomitic mudstone and dolostone, whereas the terrigenous component contains well-rounded coarse quartz grains, angular fine quartz clasts, rare fine feldspar clasts, lithic clasts, and carbonaceous mica-rich matrix (Fig. 2C). Phosphate occurs as a fine agglomerate of cryptocrystalline apatite in matrix. This rock forms very restricted beds frequently separated by erosion surfaces at the bottom and it is generally overlaid by finer-grained sequence enriched in organic matter. Given these very particular features, this layer is an excellent structural and stratigraphic marker and was used to balance cross sections and the 3D model.

Hydrothermal dolomitic breccia: Bonsucesso Zn-Pb mineralization

The Zn and Pb orebodies of the Bonsucesso deposit are hosted in a hydrothermal dolomitic breccia. There are two mineralized zones. The upper zone occurs in the hanging wall along the fault plane, below the carbonate mudstone layer and above the Serra do Garrote carbonaceous phyllite. Its basal contact with the latter has less to no shearing. In the footwall, the mineralized zone also extends along the fault plane, above the carbonate metamudstone package and below the Serra do Garrote phyllite, and its contact with the latter exhibits abundant shearing structures (Fig. 3).

The host rock is a hydrothermally brecciated dolostone with intense veining by white coarse dolomite and sulfides. The length of the deposit along the strike is approximately 4,000 m, but brownfield exploration programs have demonstrated a potential for extension. Breccia zone thickness varies through the strike, and mineralized zones within it may vary as well. The faulting process is a major permeability control, and deformation is heterogeneous. In general, the mineralized zone is hosted in a 50-m brecciated dolomite, whose extension is controlled by faults.
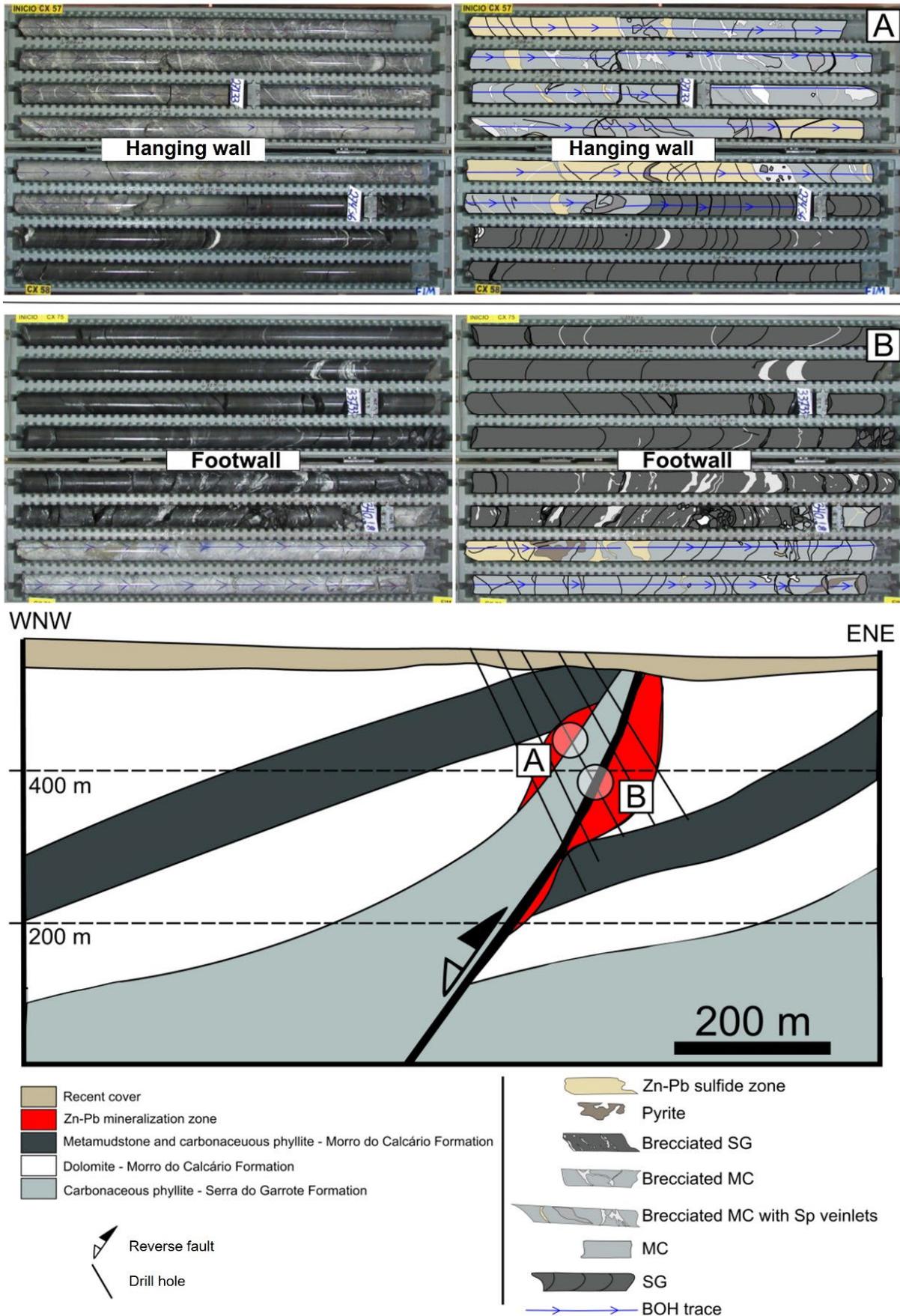
SG: Serra do Garrote Formation; MC: Morro do Calcário Formation; BOH: bottom of hole.

Figure 3. The contact relationship between Zn-Pb mineralization zones and host rocks in the fault blocks. Circles A and B represent the approximate positions of the drill cores along the same drill hole. (A) Contact between the mineralized zone and the SG rocks in the hanging wall block is a transition contact. (B) Contact between SG rocks and the mineralized zone is marked strong shearing in the footwall block. Occurrence of intense veining by quartz and minor calcite also shows that this is the slip surface (thick black trace). At left, cases containing the drill cores. At right, the schematic representation highlights the main features of the rocks. At bottom, the geological cross section of the Bonsucesso Zn-Pb sulfide deposit (see Fig. 7 for its location).

Two prevailing mineralization types have been described: breccia with angular dolostone-clasts surrounded by sphalerite (Sp), galena (Gn), and gangue minerals (Py, white dolomite, and quartz), and veins of Sp and Gn. The mineralogy of the Bonsucesso is relatively simple. Mineralization is comprised of Sp, Gn, and gangue minerals such as Py, white dolomite, and quartz, with scattered punctuations of pyrobitumen. Sp color ranges from gray to dark gray and pale yellow to amber. The former represents the major Zn sulfide component of the deposit, and the latter is often related to late and coarser Sp mineralization (Fig. 4).

# MINERALIZATION AND STRUCTURES AT THE BONSUCESSO DEPOSIT

Ore mineralogy

Colloform Py is frequently observed as a sulfide phase, with texture indicating replacement by Sp and Gn. Mineralization by veining is marked by the injection of Sp and Gn at high angles, often in extensional veins. A well-formed Py and the replacement of sulfide phases by carbonate minerals and quartz are also common (Fig. 4).

WDS compositional maps (Fig. 5) show an iron (Fe) zonation in carbonate minerals with an increase toward the center of
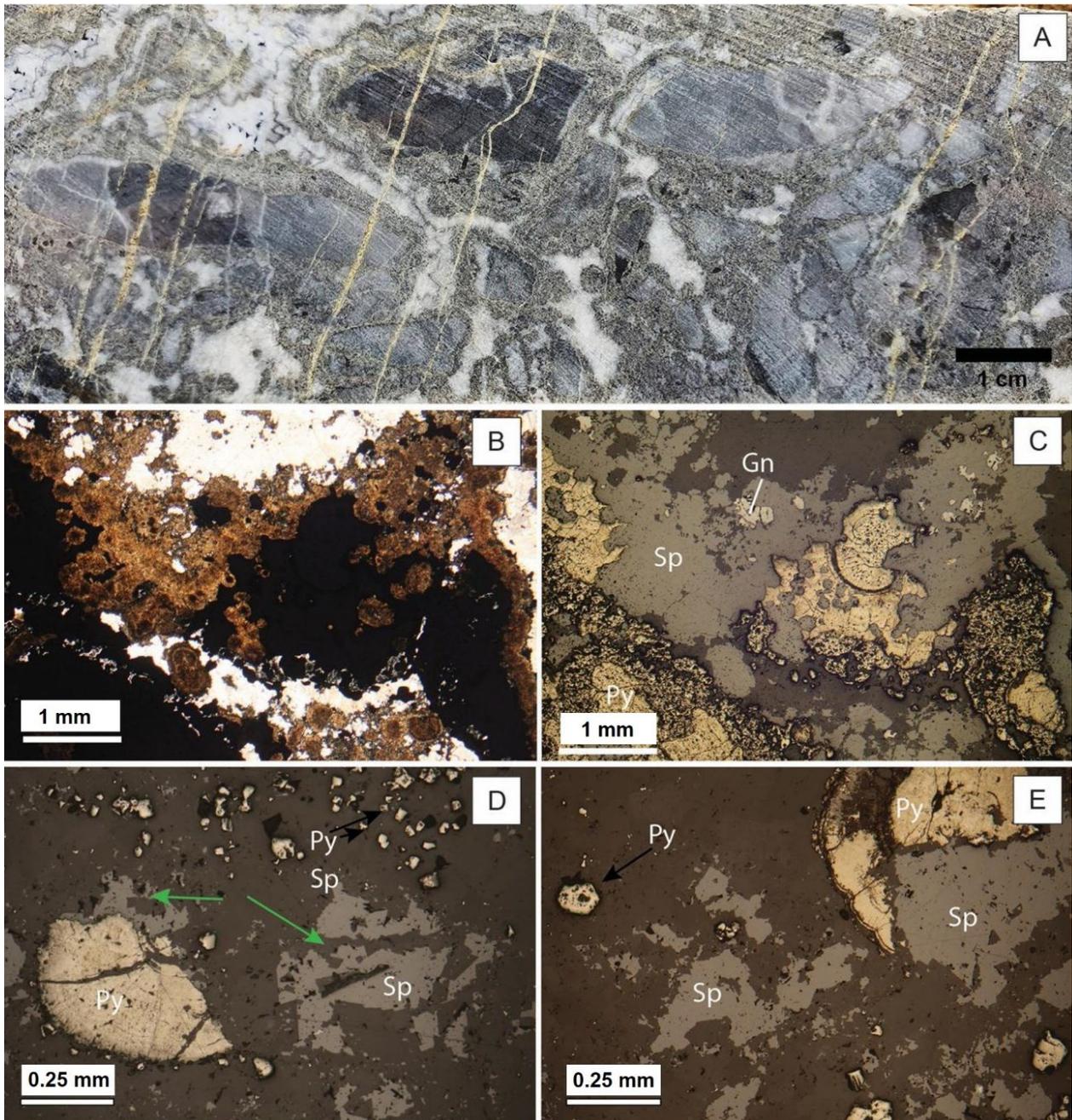
Sp: sphalerite; Gn: galena; Py: pyrite.

Figure 4. (A) Hydrothermal dolomitic breccia almost entirely cemented by gray and yellow colloform Sp and cut by late Sp-bearing veinlets. Sulfide and gangue-minerals, mainly dolomite, under transmitted (B) and reflected (C) light, showing the filling of inter-fragment open spaces in dolomitic breccia. (D) Sp replaced colloform Py. The same Sp is later replaced by carbonate mineral (rhombohedral crystal is indicated by green arrows). (E) Another example of Sp replacing early phase of colloform Py. Both thin sections contain a late phase of euhedral Py.
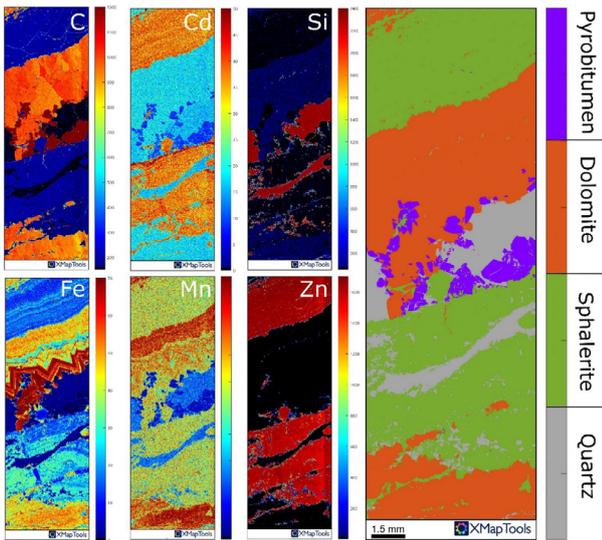
C: carbon; Cd: cadmium; Si: silica; Fe: iron; Mn: manganese; Zn: zinc.

Figure 5. Paragenetic map and compositional maps of an extensional mineralized vein (see location of map on Fig. 6).

a Sp-bearing vein. For Fe, there is also a slight banding in Sp. In regard to manganese (Mn), there is a decrease toward the center of the vein. The cadmium component is strictly related to Sp. Si and carbon (C) are concentrated at the core of the analyzed vein.

Monteiro (2002) documented the existence of oil inclusions in sulfide phases related to mineralization in the Vazante Belt. At the Bonsucesso deposit, the occurrence of pyrobitumen among hydrothermal mineral phases is very common. The relationship of pyrobitumen with Sp is clearer at the microscopic scale where Sp-bearing veins show oil residues in direct contact with Zn sulfide. At the mesoscale, it is also possible to see specks and needle-like pyrobitumen among gangue minerals (Fig. 6).

Paragenetic sequence

Table 1 summarizes the paragenetic sequence of sulfides at the Bonsucesso deposit. As this study was not able to detail the occurrence of phases of quartz, dolomite, and other gangue minerals, we assume a widespread distribution of these minerals in all major fluid injection events.
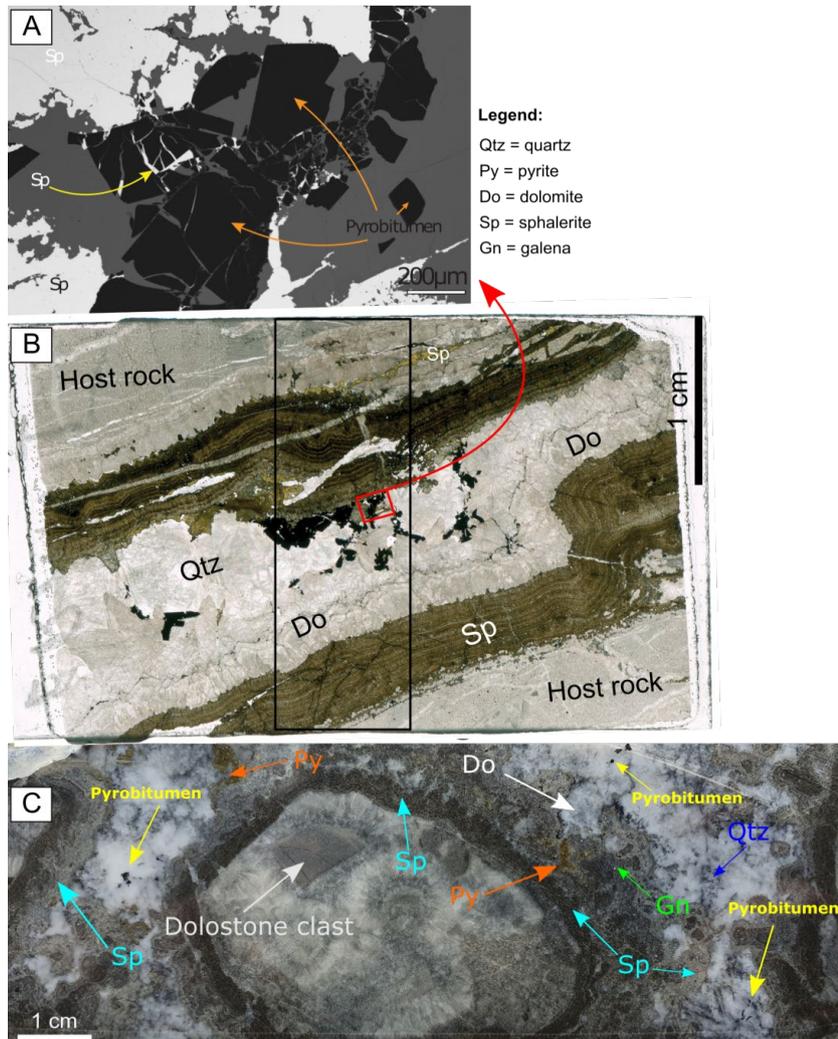

Figure 6. Zn-Pb sulfide mineralization and its relation with pyrobitumen. (A) Back scattered electron image showing pyrobitumen in contact with Sp. Red arrow indicates location of EDS image in the thin section (B). Oil residues occur mainly in the core of the vein and make contact with ore minerals and gangue minerals. Bands of Sp suggest multiple fluid injection during vein growth. Comb texture of crystals indicates extension without a shearing component. *Black rectangle = location of compositional maps.* (C) Core sample showing the main phase of mineralization (colloform Sp and minor Gn) and gangue minerals (white dolomite, quartz, and Py). There are still some angular dolostone clasts completely involved by hydrothermal minerals. Some specks and needle-like occurrences of pyrobitumen are clearly visible within masses of white dolomite.

Table 1. Paragenetic sequence of Bonsucesso deposit sulfides.

	Pre-ore	Main mineralization	Late mineralization
Colloform pyrite	▓▓		
Euhedral pyrite			▓▓
Sphalerite		▓▓	
Galena		▓▓	
Oil	▓▓		

Structures

Faults

Faults at the Bonsucesso deposit include NNW-striking and WSW dipping reverse fault and ESE –WNW and WSW – ENE high-angle transcurrent faults (Fig. 7).

The reverse fault juxtaposed metasedimentary rocks of the Serra do Garrote Formation against dolomite rocks of the Morro do Calcário Formation (Fig. 7). The sense of motion provided by slickenlines indicates that the fault is reverse (Fig. 8). The NNW reverse fault comprises a smoothly curved surface that delineates the occurrence of Zn-Pb mineralization. Fault-morphology was defined by the limits of fault-core, damage zone, and hydrothermal brecciation zone. Slickenlines were measured at fault planes only in phyllite and indicate the top-to-east reverse motion (Fig. 9). Coupled with slickenline vectors, the duplication of carbonate mudstone layers was also a guide to determine the kinematics as reverse.

Using the likely displaced mineralized zones (Bonsucesso and Ambrósia Norte deposits) intersected on both sides of these transcurrent faults, offset was estimated to be around 200 m with a dextral shear sense at the Santa Rita Creek fault (south end of Bonsucesso deposit). At the current northern end of Bonsucesso deposit, the NNW reverse fault is truncated by strike-slip fault and offset to west. More district-scale field work addressing these faults is fundamental to determine more precisely the kinematics of the strike-slip component and also a normal dip-slip component cannot be ruled out.

Folds

Anticlines and synclines were defined by measurements of bedding planes at both hanging and footwall blocks. Recrystallization of primary minerals is incipient and bedding is parallel to the first tectonic cleavage (S1). This bedding-parallel foliation is spaced and marked by fine sericite and quartz bands in phyllites and by sericite, quartz, and carbonate clasts in metamudstone.

Major folds at Bonsucesso deposit are gently open folds with low-angle axis plunging to southwest. The position of the anticline at the south sector matches the occurrence of thrusted basal rocks of the Serra do Garrote Formation on shallower levels. At the central sector, the occurrence of phyllites of the Serra do Garrote Formation is deeper and matches the syncline's hinge zone (Fig. 7).

Isoclinal folds were observed in phyllites of the Serra do Garrote Formation and comprise a group of centimeter to meter folds characterized by folding of bedding with fold axis plunging around 10° to either SE or NW. Localized isoclinal folds related to shear zones are also observed (Fig. 10). At Bonsucesso deposit, the axial cleavage parallel to regional isoclinal folds (Monteiro *et al.* 2006) was not recognized.

Mineralized veins

Mineralization in veins occurs mainly in high-angle veins within the hydrothermal breccia zone. Although they do not correspond to the most volumetric component of mineralization (i.e., Zn-Pb sulfides filling breccia-matrix), these high-angle veins are mostly extensional veins grown by open-space filling process without shear (Fig. 11). There are also Sp-bearing veins with lower dips.

A possible metallogenic model: Discussion

Timing of mineralization

The zinc and lead mineralization of the Bonsucesso deposit is hosted in a hydrothermal breccia. The origin of this breccia is directly linked to the faulting process because the presence of this fault-related breccia defines the mineralized zone.

The present setting of rocks is the result of a reverse fault that emplaced phyllites of the Serra do Garrote Formation between dolomite rocks of the Morro do Calcário Formation and generated a stratigraphic duplication attested by the repetition of carbonate mudstone in both fault blocks.

Another important aspect to understand the evolution of the deposit is the common absence of shearing between the base of hanging wall mineralized breccia and top of Serra do Garrote phyllite. Additionally, many drill core intervals show a gradual transition from the dolomite unit to the lower siliciclastic unit (Serra do Garrote Formation). In contrast, the contact between the base of the Serra do Garrote phyllite and the top of the footwall-mineralized breccia exhibits strong shearing structures, with evidence of top-to-east sense of motion. Furthermore, the Serra do Garrote Formation rocks do not bear any ore mineralization, and the hydrothermal minerals occurring within this unit are only veining by quartz and calcite around the reverse fault, but there is no replacement by ore minerals or any sign of interaction with the Zn-Pb mineralizing fluids (e.g., a hydrothermal halo).

Regarding the structural evolution of the Bonsucesso deposit, three different scenarios (Table 2) are suggested for the formation of the Zn-Pb mineralization: mineralization was formed during local extensional regime, and before or during basin inversion completion, Bonsucesso mineralization was generated during a local and regional compressive state regime during basin inversion. Its high angle fault is the result of reactivation of inherited normal faults. Phyllite between fault blocks is the result of progressive advance of the thrust front, and controlling structures and mineralization were formed during local and regional compression regime. Bonsucesso high-angle fault was primarily of low angle and then rotated to the current position.

Our preferred scenario is the mineralization formed during local extensional regime before or during basin inversion (Fig. 12).
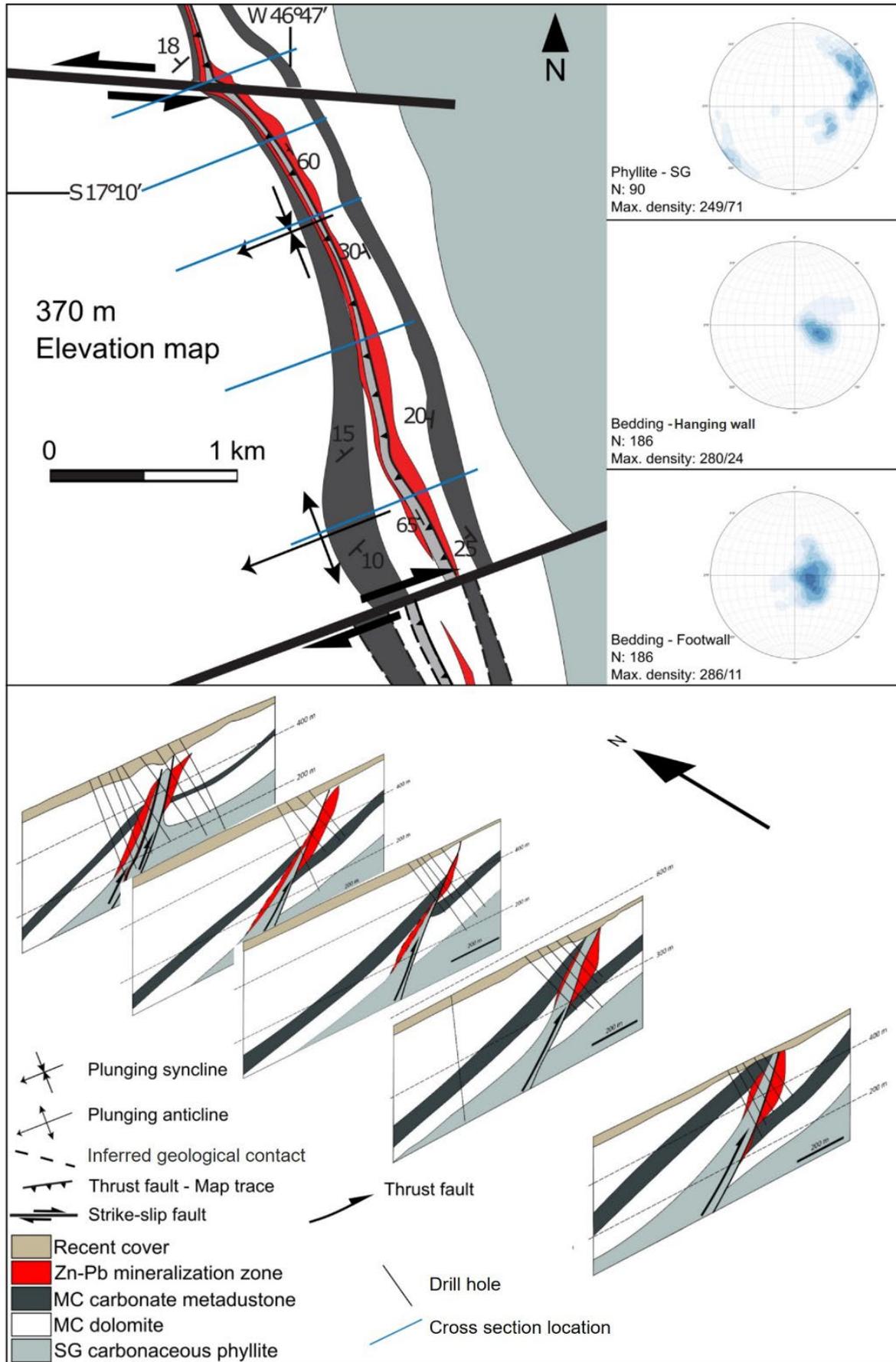
Figure 7. The 370-m-elevation geological map showing the mineralized reverse fault truncated by strike-slip faults. At upper right, lower-hemisphere equal-area stereographic projections of the structures in the Bonsucesso area. From top to bottom: "Phyllite-SG" stereonet shows the attitude of Serra do Garrote (SG) Formation rocks emplaced between the two fault blocks; the other two stereonets show measurements of bedding on hanging wall and footwall blocks. In the lower part, a perspective view of geological cross sections along the entire Bonsucesso Zn-Pb sulfide deposit. The second cross section from south to north contains a drill hole positioned farther to west. This drill hole has confirmed the continuation of the stratigraphic pile and the lower dip of the rocks at this location, which is distant from the reverse fault zone.
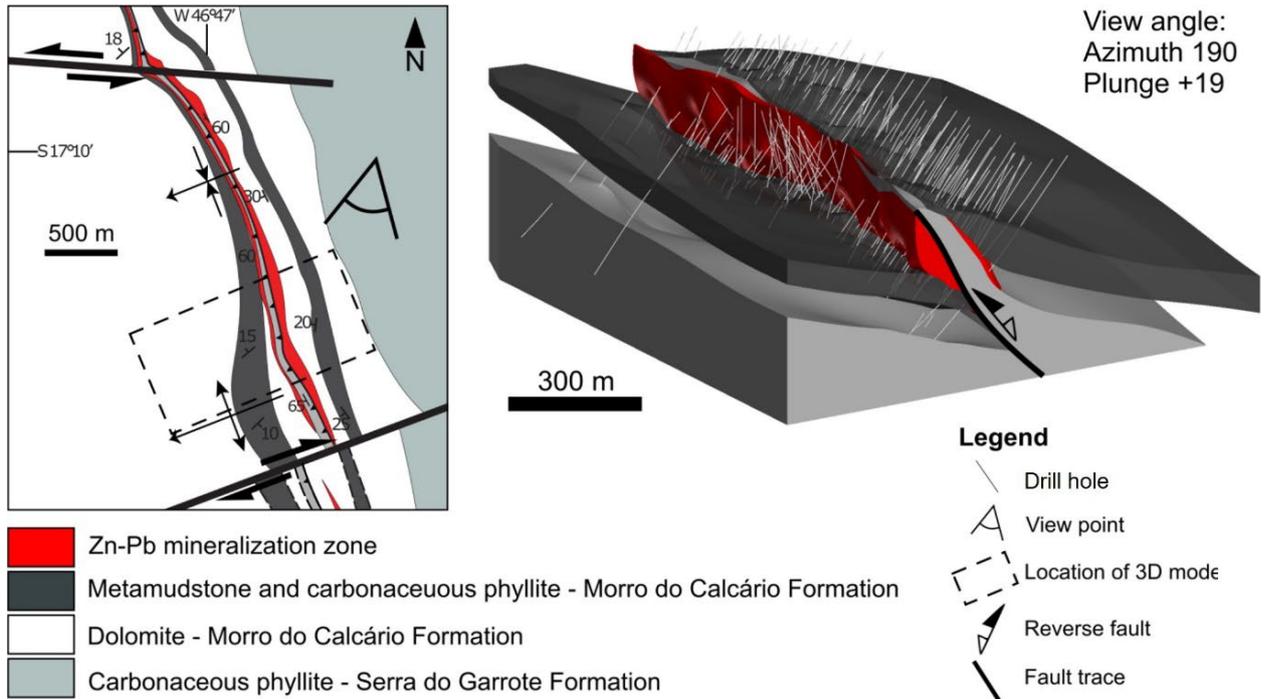
Figure 8. 3-D model of the Bonsucesso Zn-Pb sulfide deposit. The dolomite rocks were taken out to ease the visualization of the geometry of the ore zone. Drill holes have crossed the carbonate metamudstone in the hanging wall, the upper breccia zone, the phyllites of the Serra do Garrote Formation emplaced by fault, the mineralization in the footwall, once again the carbonate metamudstone, but in the footwall, and, finally, the Serra do Garrote Formation rocks once again. Note that the upper mineralization zone is smaller, and along the deposit, its geometry is more irregular. At the extreme north of the geological map, the main mineralization is now located in the hanging wall block.
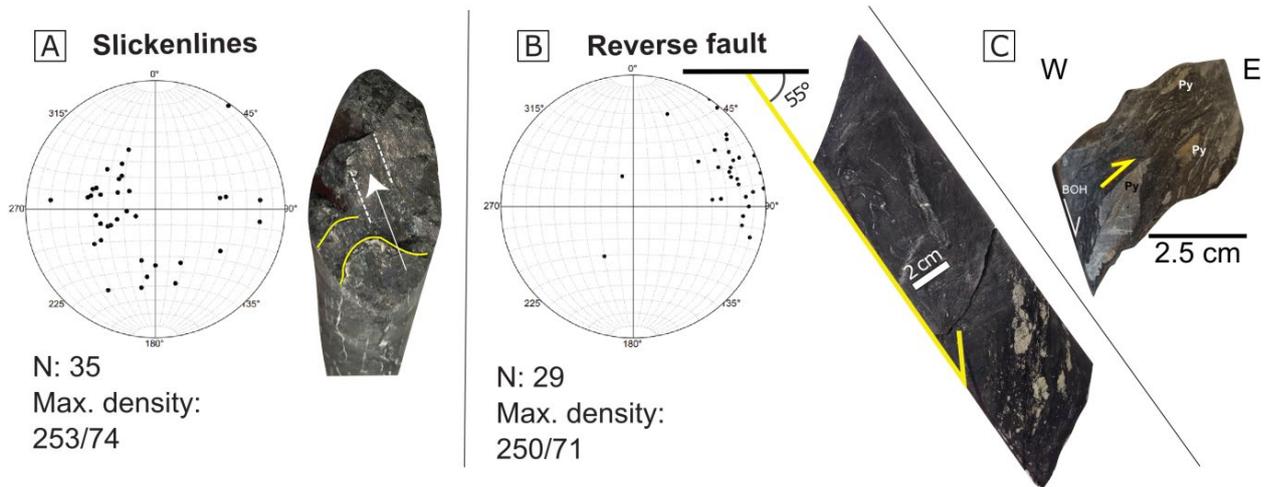
Py: pyrite; BOH: bottom of hole.
Figure 9. (A) Slickenlines on reverse fault surface. Lineations (white dashed line) mark the direction of movement. The sense of the steps (yellow lines) indicates this side of the fault moved down and the other side moved up (sense of movement indicated by white arrow). At left, lower-hemisphere equal-area stereographic projection of the slickenlines. (B) Reverse fault plane. Drill core showing intense shearing and veining by quartz and minor calcite at the fault zone. At left, lower-hemisphere equal-area stereographic projection of poles to fault planes. (C) Sigmoid dolomite clast indicates movement to the east. The clast is contained within a fault gauge zone. Also, some deformed Py clasts at the right half of the core sample. There is also some early Py inside the dolomite clast.

The final setting of the Bonsucesso Zn-Pb sulfide deposit may seem simple (T4, Fig. 12), but to reach this geometry, a more complex evolution is necessary. The amount of Serra do Garrote rocks situated above the cutoff point is greater than the displacement required to only reconnect the marker beds (T3, Fig. 12) if the cross section is restored. Thus, a greater extension (T2, Fig. 12) would be needed to resolve the final geometry. This model is capable of combining an explanation for the final geometry, the formation of a high-angle extensional ore-controlling structure, and its associated high-angle vein system. Segmentation of ore zones would be a post-ore event. Also, the same slip surface of the normal movement may not be the slip surface of the inversion movement. This could explain some features as the preservation of contacts between the mineralized zone and the basal unit (Serra do Garrote Formation) without shearing (Fig. 3) in the hanging wall block.
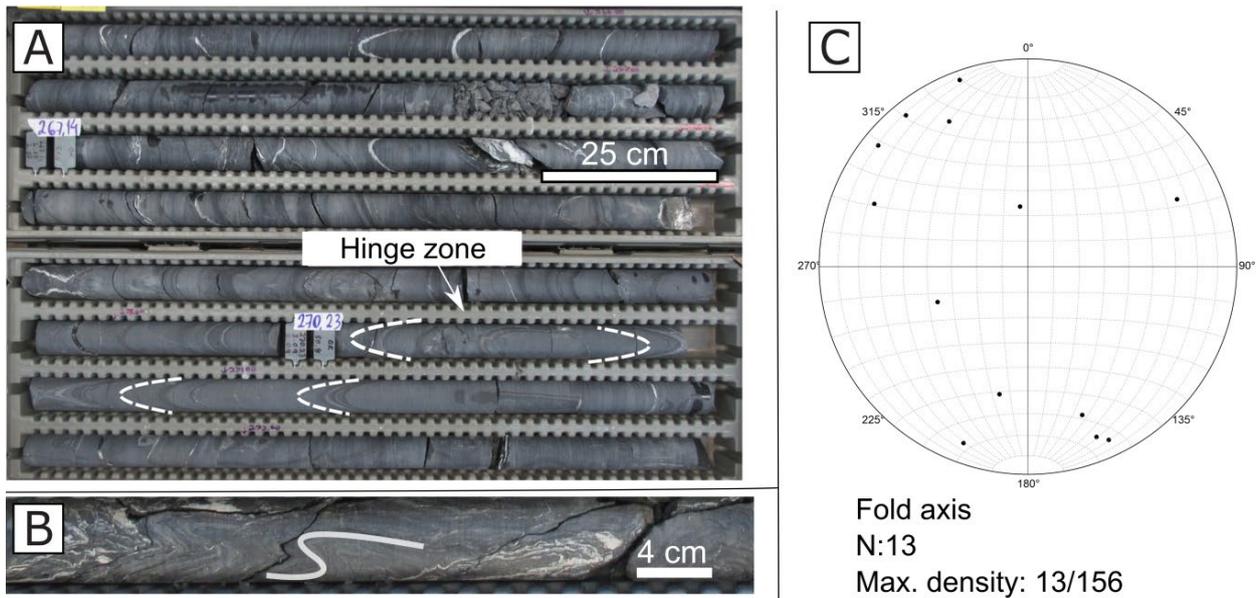
Figure 10. Folds on phyllites of the Serra do Garrote Formation inserted between Morro do Calcário faulted blocks. (A) Hinge zone of a metric fold. Dashed white lines indicate planes of intersection of bedding surfaces with core samples. (B) Fault-related isoclinal fold within the shear zone. (C) Low-plunge axis of isoclinal folds. Lower-hemisphere equal-area stereographic projection of fold axis.
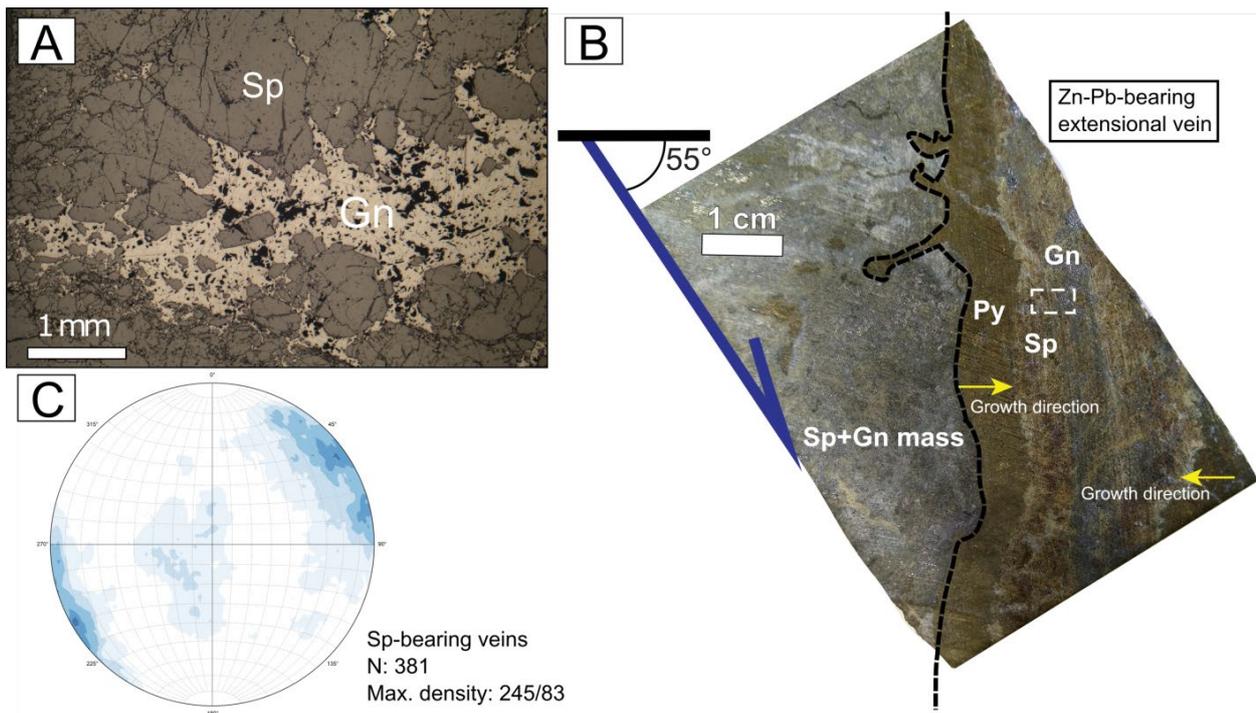

Figure 11. High-angle extensional mineralized veins. (A) Photomicrograph of Zn and Pb sulfides from the core of the vein. At this scale, it is not possible to distinguish any crystallization order or zonation. (B) The vein is composed of borders of Py with a Sp and Gn core. Growth direction is perpendicular to fracture and indicated by yellow arrows. Black dashed lines represent the vein limits in contact with a mass comprised of Sp and Gn. White dashed polygon indicates the location of the photomicrograph. (C) Lower-hemisphere equal-area stereographic projection of poles of Sp-bearing veins showing at least two major families: (i) high-angle veins and (ii) low to middle dip angle veins. The strike orientation of veins is subparallel to the Bonsucesso-fault strike. The blue arrow indicates the bottom of the drill hole and its dip.

Another important factor is the mechanical contrast between the dolomite rocks and the rocks of siliciclastic origin. The dolostone unit is more prone to fracturing and its rocks are made up of more chemically reactive minerals (essentially dolomite), whereas the more ductile basal units may have favored the normal dragging and set multiple likely planes of slip.

One final and brief comment on the nature of the mineralizing fluids is important. Besides the secondary porosity and permeability enhanced by the Bonsucesso fault system,

Table 2. Different scenarios suggested for the formation of the Bonsucesso deposit Zn-Pb mineralization.

Scenario	Elements to support this hypothesis	Elements to argue against this hypothesis
Mineralization formed during local extensional regime before or during basin inversion	High-angle of the controlling fault; High-angle of mineralized veins; High-angle extensional mineralized veins with no shear; Normal faults are efficient conduits for hydrothermal flux (Sibson 2000) and in many cases form barriers for hydrocarbon accumulations (Hardman and Booth 1991); Disposition of mineralized breccias into two segments divided by an allochthonous phyllite. Emplacement of Serra do Garrote Formation rocks between carbonate rocks of Morro do Calcário occurred after main mineralization process, once the latter are deformed by the former.	Which major regional extensional event was responsible for mineralization prior to complete inversion? Layers in both fault blocks show minimal thickness alteration when considering their association with normal faults related to Vazante Group deposition. Therefore, it appears that the extension occurred after the deposition of the Vazante Group. However, a significant event capable of causing such extension before the completion of basin inversion is the synorogenic formation of the foreland basin, which hosts the Bambuí Group sediments (Brito Neves *et al.* 1996, Almeida *et al.* 2000, Alkmim 2004, Reis and Alkmim 2015). Reis *et al.* (2017) have described extensive normal faulting as a result of a forebulge uplift in the east. Nevertheless, the effects of this process on the Vazante Group rocks remain unclear. Additionally, similar to the Vazante Group, the Bambuí sediments were also affected by thin-skinned tectonics, and large thrust faults are identifiable along the foreland sedimentary sequence (Reis and Suss 2016, Reis *et al.* 2017).
Mineralization generated during a local and regional compressive state regime during basin inversion	Similar to the previous hypothesis, the fault promoted an increase in rock permeability within the damage zone and facilitated the connection of overpressured fluids from sealed reservoirs. These fluids then migrated to a precipitation site where favorable geochemical conditions were present. The inversion of inherited normal faults is often invoked to explain the formation of certain mineral deposits controlled by high-angle reverse faults, as described in Sibson's model of fault-valve (Sibson *et al.* 1988). This is because, under compressional conditions (horizontal sigma 1), the development of high-angle thrust faults is not favorable. For these reactivations to occur, fluid pressure must exceed the lithostatic load. Consequently, significant quantities of overpressured fluids accumulate below until they are suddenly discharged to higher structural levels once this pressure threshold is reached. This cycle may be repeated multiple times, as hydrothermal mineralizing fluids can seal the cracks, leading to pressure buildup once again.	The high-angle fault itself is an issue, similar to the high-angle extensional veins. The mineralizing fault-valve process is well-known in orogenic gold deposits, where controlling high-angle faults often extend deep into the seismogenic crustal limit (Sibson *et al.* 1988). However, there is currently no evidence to suggest that the Bonsucesso fault or any thrust fault in the Vazante Belt has such deep extensions.
Controlling structures and mineralization were formed during local and regional compression regime	The mineralized zones are controlled by a reverse fault. The high angle of the controlling fault may be attributed to a rotation caused by the absorption of regional shortening.	Low-angle thrust faults are commonly associated with high dilation zones. Mineralized veins at the Bonsucesso deposit do not exhibit shear. Even when veins and fault planes are back-rotated to a position close to a common low-angle thrust fault, the mean veining attitude does not align with the expected Riedel-shear fractures.

a sulfide mineralization needs the right chemical conditions to form. In simple terms, a source of sulfur, a source of metals, and the reductant environment/agent are required. The complete understanding of this process is beyond the scope of this study, but we have presented here some data related to the mineralogy of the deposit and the presence of oil residues is intimately associated with the ore and gangue minerals. Then, we suggest that the Bonsucesso fault system may have some connection with oil reservoirs prior to the Zn-Pb sulfide mineralization. Brines (source of sulfur and metals) moving through different reservoirs encountered the mobile reductant agent (hydrocarbons) in the Bonsucesso fault system and precipitation took place.

Deformation history

Sequence of deformation events at Bonsucesso deposit is summarized in Table 3.

Generation of normal faults with influx of hydrothermal mineralizing fluids occurred in early stages of collision (D1). As the Brasília thrust front advanced (D2), S1 cleavage and isoclinal folding were formed together with thrust faults and with subordinate mineralization. The Serra do Garrote phyllite was emplaced between the carbonate rocks from the Morro do Calcário Formation during this phase. Stage D3 is marked by a strong strike-slip component and open-folding. A final extensive regime characterized by normal faults with small displacement or only joints is well recognized regionally

(Pinho 1990, Rostirolla *et al.* 2002, Cordeiro *et al.* 2018) but it was not described at the scale of the Bonsucesso deposit.

Open folds with SW-NE axis may be contractional fault-related folds, resulting from different depths of detachment and displacement transfer with a strike-slip component (i.e., a mechanism of drag folding). These interacting faults (transcurrent and thrust faults) may also control the emergence of deeper layers and also segment orebodies.
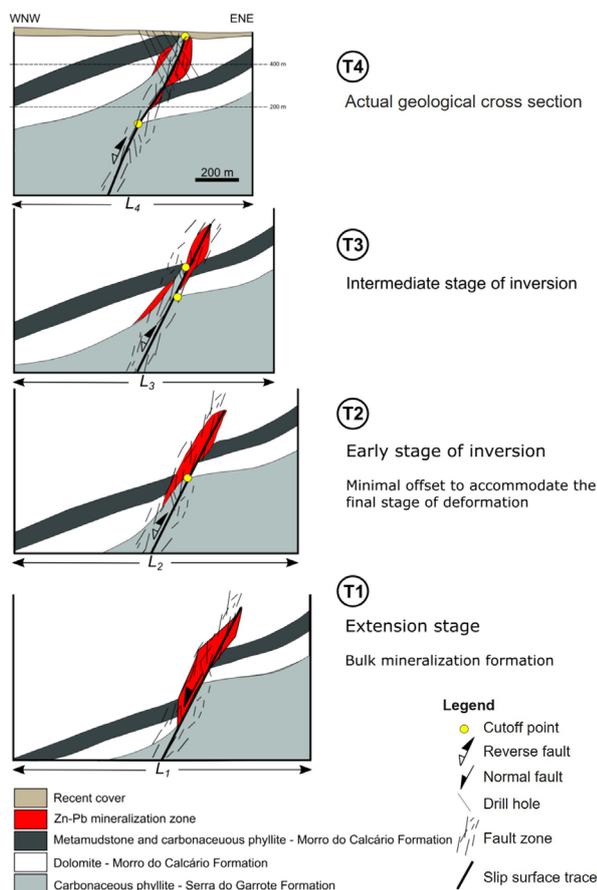

Figure 12. Evolution model for the Bonsucesso Zn-Pb sulfide deposit. To accommodate the final geometry of the deposit (T4), a single thrust fault is not enough to explain the amount of SG rocks emplaced. If the dip of layers is preserved and the marker beds are reconnected (T3), there is some SG rocks left out, thus a greater extension (L2) is needed to reach a point of minimal offset to compensate for the total displacement (T2), considering that the movement is mainly down-dip during extension and up-dip during inversion. Proposed metallogenic model favors a mineralization phase related to an early extension (T1). Geometry of SG rocks in the hanging wall block presented in T1 and T2 are probably due to drag folds associated with normal fault zone.

Comparison between the Bonsucesso deposit and the other Vazante Belt deposits

The Morro Agudo deposit is hosted mainly in a doloarenite layer, whose matrix was replaced by Sp with subordinate mineralization in fault-dolomite breccia and intraformational dolomite breccia and also replaced stratiform orebodies in carbonate lenses within metapelites of the Serra da Lapa Formation (Dardenne and Freitas-Silva 1999, Misi *et al.* 1999, 2005, 2014, Cunha *et al.* 2000, 2007, Cordeiro *et al.* 2018).

Mineralization in the Morro Agudo deposit is interpreted to be related with fluids ascending from a main normal fault located in the east limit of the deposit (Dardenne and Freitas-Silva 1999, Misi *et al.* 1999, 2005, Cunha *et al.* 2000, 2007). Likewise, Cunha *et al.* (2000) and Misi et al. (2005) showed a cooling pattern in homogenization temperature, salinity, and isotopic data toward deeper and distal sectors from the main fault. Nonetheless, there is a set of smaller normal faults with an oblique component which offset the orebodies and host rocks (Cordeiro *et al.* 2018). These faults are ore modifiers and have the same attitude of the main fault and also the main fault does not feature any clue of hydrothermal alteration expected to a feeder zone. Therefore, the referred structure would be only other later but larger normal fault modifying the whole rock sequence (Cordeiro *et al.* 2018). So, without contradicting the recognized cooling pattern, Cordeiro *et al.* (2018) call for any conduit capable of mobilize fluids before faulting into smaller blocks and that a major feeder may have been eroded or simply not intersected by drilling yet. Hence, mineralization at the Morro Agudo deposit took place before basin inversion.

In this sense, even if Morro Agudo had multiple phases of ore fluids injection, they all point to an early bulk mineralization event that happened before overprinting of compressive structures and may be contemporaneous with a hypothesis of pre-thrust mineralization of Bonsucesso. Cordeiro *et al.* (2018) discussed that there is a strong, although overlooked, strike-slip component in Morro Agudo, possibly related to the collisions between the Amazonian, São Francisco, and Paranapanema paleoplates (Brito Neves and Fuck 2013).

The Ambrósia, Ambrósia Sul, and Bonsucesso deposits form an aligned cluster of Zn-Pb mineralization (Fig. 13) with minor offset by strike-slip fault and may constitute an earlier permeable normal fault system with high influx of hydrothermal fluids later overprinted by thrusting.

The Ambrósia Sul deposit represents another Zn-Pb sulfide deposit formed during an early extensional event and is located

Table 3. Deformational phases of the Bonsucesso deposit.

D0	D1	D2	D3	D4
Bedding	Flexurally induced normal faults	Thrust faults, S1 cleavage, Isoclinal folding with low plunge to NW and SE	Open folds SW-NE, Strike-slip faults	Late normal faults with small offset (Pinho *et al.* 1990, Rostirolla *et al.* 2002, Cordeiro *et al.* 2018)
	Main mineralization *Local extension/foreland*	Late mineralization	Mineralization is deformed	
Passive margin	**Compressive regime/Brasília belt thrust front**			

Stage 1
Mineralization in flexurally
induced normal faults

Stage 2
Deformation of mineralization
during basin inversion

Hydrothermal dolomite breccia with Zn-Pb sulfide ore
(surface projection)

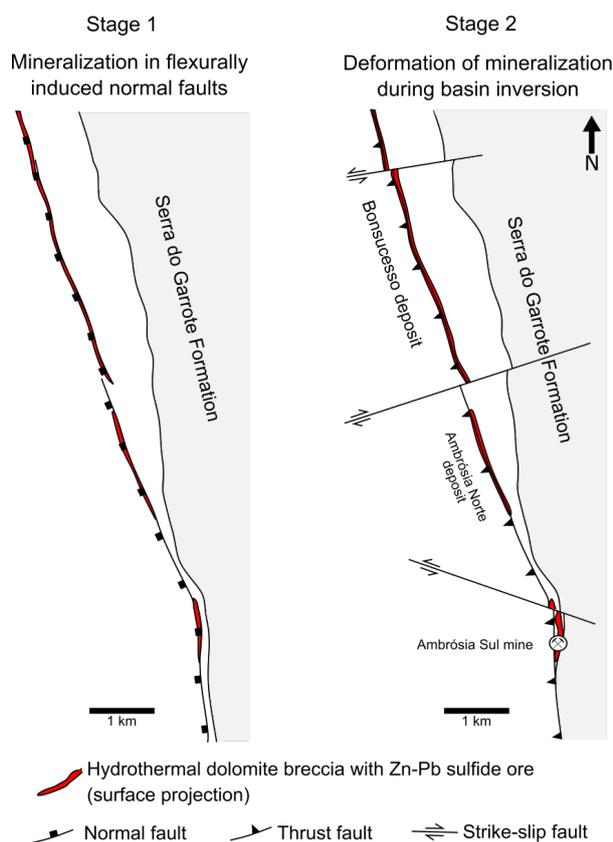Normal fault   Thrust fault   Strike-slip fault

Figure 13. Simplified genetic model of mineralization-related structures at the Bonsucesso, Ambrósia Norte, and Ambrosia Sul deposits. Stage 1: Extensional fault system took place and formed the bulk mineralization of all three deposits. Stage II: Advance of thrust front took over ancient extensive structures, formation of reverse faults, and strike-slip displacements.

in the same trend 5 km southward from the Bonsucesso deposit. According to Botura Neto and Danderfer Filho (2022), mineralization is associated with a syn-orogenic extension during formation of Bambuí Group foreland basin and normal faulting is related to forebulge uplift (Reis *et al.* 2017). Although the emergence of basal layers in the Ambrósia Sul deposit is not as evident as in the Bonsucesso deposit, Neto (2018) interpreted the high-angle mineralized veins formed during a compressive regime cut by late low-angle thrust faults associated with minor Sp-bearing veins.

The Ambrósia Norte Zn-Pb deposit, also known simply as Ambrósia Zn-Pb deposit, is associated with epigenetic processes (Monteiro *et al.* 2006) and is also controlled by a high-angle fault. This deposit is located just 1.5 km to the south from Bonsucesso and its mineralization style (Monteiro *et al.* 2006, 2007) is similar to Bonsucesso. These deposits are separated by a transcurrent fault zone and projection of their mineralization onto the surface shows a 200 m relative offset if it is assumed that they are controlled by the same fault.

The mineralization of Vazante non-sulfide Zn deposit is controlled by a 12 km long fault zone trending northeast and dipping 60° to northwest (Monteiro *et al.* 2007). This major shear zone also shows a complex deformation history (Dardenne 1974, Pinho 1990, Rostirolla *et al.* 2002) and an important role in the mineralization process as the main conduit, besides many particular features involving willemite formation and hydrothermal alteration processes unequal in the world (Monteiro *et al.* 1999).

Bonsucesso deposit × Tectonic settings of MVT Pb-Zn deposits on Earth history

As discussed by Leach *et al.* (2010), the tectonic setting of ore deposits is the conjuncture where they are formed and eventually destroyed. Also, this moment on an evolving Earth "determines the host-rock type, ore controls, temperature, and pressure of the depositional processes, as well as the survivability of the deposit during tectonic recycling" (Leach *et al.* 2010).

According to Bradley and Leach (2003), the most suitable environments for MVT mineralization are former passive margin platform carbonates that ended up beneath foreland basin deposits generated during the collisional orogeny. After orogeny has ceased, a hydrologic flux of basinal brines would be favorable, which percolates through the normal faults induced by crustal flexure occurred during the formation of accommodation space of the foreland basin (Leach *et al.* 2010).

The way that Bonsucesso's mineralization fits in this model is that it is hosted in former passive margin platform carbonates beneath a foreland basin; it is controlled by high-angle dilatational structure; and the salinity, isotopic, and homogenization temperatures of near-by deposits have an upper crustal/basinal signature (Monteiro *et al.* 2006, 2007). Although, Vazante Group has undergone a shortening process that lasted longer than the foreland basin deposition process and the latter was also involved in the thin-skinned tectonics as it was added to external domains of Brasília Belt during the late stages of assembly of West Gondwana (Alkmim *et al.* 1996, 2001, Brito Neves *et al.* 1999, Pedrosa-Soares *et al.* 2001, 2007, Alkmim 2004, Brito Neves 2004, Valeriano *et al.* 2004, Caxito *et al.* 2014, Reis and Alkmim 2015). Finally, an extensional phase of mineralization before basin inversion with some late remobilization also agrees with Misi *et al.* (1999, 2005, 2014), Monteiro *et al.* (2006, 2007), Cunha *et al.* (2000, 2007), and Dardenne and Freitas-Silva (1999) proposals for Morro Agudo, Ambrosia, Fagundes, and Vazante deposits.

Implications for mineral exploration

The Zn-Pb deposits in the Vazante belt are intimately linked to fault zones (Dardenne and Freitas-Silva 1999, Monteiro 2002, Misi *et al.* 2005, Monteiro *et al.* 2006, Cordeiro *et al.* 2018). The flow of metal-rich fluids occurred throughout the Vazante basin, and dilatational structures functioned as avenues for them to be redistributed along the strike and crystallize where chemical conditions were adequate. Contrasting rheological properties of brittle dolomite rocks from Morro do Calcário Formation and more ductile phyllites from the Serra do Garrote Formation could have transformed Vazante Group in a giant fluid trap, where the permeability in carbonate rocks increased by faulting and different reservoirs were allowed to interact.

Historically, mineral exploration programs evolved through the follow-up of outstanding geochemical anomalies in the regolith (e.g., metal rich gossan). In the Paracatu and Vazante regions, it was not different; all major orebodies currently mined were once cropping out. In the entire region, the Bonsucesso deposit is the first orebody discovered lying under a 30-m-thick pile of recent sediments. Although, its discovery is particularly

connected with a gossan 1 km to south slightly with the same strike (Ambrósia Norte) and targeted for decades.

Our model presents a likely set of regional proportions involving flexurally induced normal faults later affected by thrust and strike-slip faults. High-angle reverse structures such as the Bonsucesso fault may suggest a direct link between mineralization and compressive regime, but early extensional features related to the main stage of Zn-Pb sulfide formation are identified and better fit the general model proposed for most of the Vazante Belt deposits of bulk mineralization pre-inversion (Misi *et al.* 2005, 2014, Monteiro *et al.* 2006, 2007).

High-angle fault-zones dipping to the west (the general dip of the thrust belt) may be mistaken as originally thrust-faults and disguise other exploration opportunities such as their likely own antithetic pair. Regarding that, normal antithetic faults controlling mineralization are already known in the Ambrósia Sul deposit (Botura Neto and Danderfer Filho 2022) and are poorly explored along the Vazante Belt. In addition to that, current strike-slip faults also might have worked as transfer faults during extension phase and flipped their dip as it is documented in many extension sets around the world (Milani and Davison 1988, Chorowicz 1989). Therefore, these possibilities should be taken into account when exploring in regions of interacting faults.

CONCLUSION

The Bonsucesso Zn-Pb sulfide deposit is hosted in a hydrothermal dolomitic breccia controlled by a high-angle reverse fault striking N20W and dipping 60° to SW. Mineralization is hosted mainly in the breccia-matrix, but it also occurs in high-angle extensional veins. We suggest various mineralizing scenarios, but our preferred model is that bulk mineralization was likely formed in an extensional regime setting in breccia zones controlled by flexurally induced normal faults, and mineralized zones were segmented by the injection of the more ductile basal unit (Serra do Garrote Formation). Contrasting rheological properties of brittle dolomite rocks from the Morro do Calcário Formation and ductile phyllites from the Serra do Garrote Formation acted as a fluid trap as permeability in carbonate rocks increased by faulting and different reservoirs were allowed to interact. Our model presents a possible set of regional proportions involving flexurally induced normal faults later affected by basin inversion. Thrust structures such as the Bonsucesso fault may suggest a direct link between mineralization and compressive regime, but early extensional features related to main stage of Zn-Pb sulfide formation are identified which agrees with the model proposed for most of the Vazante belt deposits of bulk mineralization pre-inversion. The mineralization process at Bonsucesso fits the model proposed by Bradley and Leach (2003) for well-known MVT provinces as follows: it is hosted in former passive margin platform carbonates beneath a foreland basin; it is controlled by high-angle dilatational structure; and the salinity, isotopic, and homogenization temperatures of near-by deposits have an upper crustal/basinal signature. The search for mineralization extensions controlled by faults should take into account an early normal faulting setting deformed by basin inversion.

ACKNOWLEDGMENTS

REFERENCES

Alkmim F.F. 2004. O que faz de um craton um cráton? O Cráton do São Francisco e as revelações almeidianas ao delimitá-lo. In: Mantesso-Neto V., Bartorelli A., Carneiro C.D.R., Brito-Neves B.B. (eds.). *Geologia do Continente Sul Americano: Evolução da obra de Fernando Flávio Marques de Almeida*. São Paulo: Beca, p. 17-35.

Alkmim F.F., Chemale Jr. F., Endo I. 1996. A deformação das coberturas proterozóicas do Cráton do São Francisco e o seu significado tectônico. *Revista Escola de Minas*, **49**:22-38.

Alkmim F.F., Marshak S., Fonseca M.A. 2001. Assembling West Gondwana in the Neoproterozoic: clues from the São Francisco craton region, Brazil. *Geology*, **29**(4):319-322. https://doi.org/10.1130/0091-7613(2001)029%3C0319:AWGITN%3E2.0.CO;2

Alkmim F.F., Martins-Neto M.A. 2012. Proterozoic first-order sedimentary sequences of the São Francisco craton, eastern Brazil. *Marine and Petroleum Geology*, **33**(1):127-139. https://doi.org/10.1016/j.marpetgeo.2011.08.011

Almeida F.F.M. 1967. Origem e evolução da Plataforma Brasileira. *Boletim 241 da Divisão de Geologia e Mineralogia, DNPM.*, **241**, 36 p.

Almeida F.F.M., Hasui Y., Fuck R.A. 1981. Brazilian structural provinces: an introduction. *Earth Sciences Review*, **17**(1-2):1-29. https://doi.org/10.1016/0012-8252(81)90003-9

Almeida F.F.M., Brito Neves B.B., Carneiro C.D.R. 2000. The origin and evolution of the South American Platform. *Earth-Science Reviews*, **50**(1-2):77-111. https://doi.org/10.1016/S0012-8252(99)00072-0

Amaral G., Kawashita K. 1967. Determinação da idade do Grupo Bambuí pelo método Rb/Sr. 21º Congresso Brasileiro de Geologia, Curitiba. *Anais*, p. 214-217.

Appold M.S., Monteiro L.V.S. 2009. Numerical modeling of hydrothermal zinc silicate and sulfide mineralization in the Vazante deposit, Brazil. *Geofluids*, **9**(2):96-115. https://doi.org/10.1111/j.1468-8123.2009.00245.x

Araujo C.E.G., Rubatto D., Hermann J., Cordani U.G., Caby R., Basei M.A.S. 2014. Ediacaran 2,500-km-long synchronous deep continental subduction in the West Gondwana Orogen. *Nature Communications*, **5**:5198. https://doi.org/10.1038/ncomms6198

Araujo V. 2019. Caracterização dos solos no depósito de zinco e chumbo de Bonsucesso, Grupo Vazante, Paracatu, Brasil. 4º Simpósio Brasileiro de Metalogenia, Gramado. *Anais*, p. 190.

Azmy K., Kendall B., Creaser R.A., Heaman L., Oliveira T.F. 2008. Global correlation of the Vazante Group, Sao Francisco Basin, Brazil: Re–Os and U–Pb radiometric age constraints. *Precambrian Research*, **164**(3-4):160-172. https://doi.org/10.1016/j.precamres.2008.05.001

Botura Neto B., Danderfer Filho A. 2022. Drill core structural analysis and extensional-contractional controls on the sulfide mineralization at the Ambrosia Sul zinc deposit, Vazante group, Western São Francisco craton, Brazil. *Journal of Structural Geology*, **154**:104474. https://doi.org/10.1016/j.jsg.2021.104474

Bradley D.C., Leach D.L. 2003. Tectonic controls of Mississippi Valley-type lead-zinc mineralization in orogenic forelands: *Mineralium Deposita*, **38**(6):652-667. https://doi.org/10.1007/s00126-003-0355-2

Brito Neves B.B. 2004. A história dos continentes: trajetórias e tramas tectônicas. In: Mantesso-Neto V., Bartorelli A., Carneiro C.D.R., Brito-Neves B.B. (Eds.). *Geologia do Continente Sul Americano: Evolução da obra de Fernando Flavio Marques de Almeida*. São Paulo: Beca, p. 123-149.

Brito Neves B.B., Campos Neto M.C., Fuck R.A. 1999. From Rodinia to Western Gondwana: an approach to the Brasiliano-Pan African cycle and orogenic collage. *Episodes*, **22**(3):155-166. https://doi.org/10.18814/epiiugs/1999/v22i3/002

Brito Neves B.B., Fuck R.A. 2013. Neoproterozoic evolution of the basement of the South-American platform. *Journal of South American. Earth Sciences*, **47**:72-89. https://doi.org/10.1016/j.jsames.2013.04.005

Brito Neves B.B., Fuck R.A. 2014. Basement of the South American platform: Half Laurentian (N_NW) + Half Gondwanan. *Precambrian Research*, **244**:75-86. https://doi.org/10.1016/j.precamres.2013.09.020

Brito Neves B.B., Fuck R.A., Pimentel M.M. 2014. The Brasiliano collage in South America: a review. *Brazilian Journal of Geology*, **44**(3):493-518. https://doi.org/10.5327/Z2317-4889201400030010

Brito Neves B.B., Winge M., Carneiro M.A. 1996. Orogêneses precedendo e Tafrogêneses sucedendo Rodínia na América do Sul. *Boletim IG-USP.Série Científica*, **27**:1-40. https://doi.org/10.11606/issn.2316-8986.v27i0p1-40

Campos Neto M.C. 1984. Geometria e fases de dobramento brasilianos superpostos no oeste de Minas Gerais. *Revista Brasileira de Geociências*, **14**(1):60-68.

Carvalho M.D.O., Valeriano C.D.M., Aguiar Neto C.C., Oliveira G.D., Heilbron M. 2019. The Vazante and Canastra groups revisited: Sm-Nd and Sr isotopes-evidence for contribution from Tonian intraplate magmatism during passive margin development along the SW São Francisco margin, Brazil. *Brazilian Journal of Geology*, **49**(1):1-16. https://doi.org/10.1590/2317-4889201920180081

Carvalho M.D.O., Valeriano C.D.M., González P.A.A., Oliveira G.D., Impiccini A. 2016. The thrust contact between the Canastra and Vazante groups in the Southern Brasília Belt: structural evolution, white mica crystallinity and implications for the Brasiliano

orogeny. *Brazilian Journal of Geology*, **46**(4):567-583. https://doi.org/10.1590/2317-4889201620160052

Catuneanu T.O., Martins-Neto M.A., Eriksson P.G. 2005. Precambrian sequence stratigraphy. *Sedimentary Geology*, **176**(1-2):67-95. https://doi.org/10.1016/j.sedgeo.2004.12.009

Caxito F.A., Uhlein A., Stevenson R., Uhlein G.J. 2014. Neoproterozoic oceanic crust remnants in the northeast Brazil. *Geology*, **42**(5):387-390. https://doi.org/10.1130/G35479.1

Chorowicz J. 1989. Transfer and transform fault zones in continental rifts: examples in the Afro-Arabian rift system. Implications of crust breaking. *Journal of African Earth Sciences (and the Middle East)*, **8**(2-4):203-214. https://doi.org/10.1016/S0899-5362(89)80025-9

Cordani U.G., Pimentel M.M., Araújo C.E.G, Basei M.A.S, Fuck R.A., Girardi V.A.V. 2013a. Was there an Ediacaran Clymene Ocean in central Brazil? *American Journal of Sciences*, **313**(6):517-539. https://doi.org/10.2475/06.2013.01

Cordani U.G., Pimentel M.M., Araújo C.E.G., Fuck R.A. 2013b. The significance of the Transbrasiliano-Kandi tectonic corridor for the amalgamation of West Gondwana. *Brazilian Journal of Geology*, **43**(3):583-597. https://doi.org/10.5327/Z2317-48892013000300012

Cordeiro P.F., Oliveira C.G., Paniago L.N., Romagna G., Santos R.V. 2018. The carbonate-hosted MVT Morro Agudo Zn-Pb deposit, central Brazil. *Ore Geology Reviews*, **101**:437-452. https://doi.org/10.1016/j.oregeorev.2018.08.002

Cowan E.J. 2014. "X-ray Plunge Projection": Understanding Structural Geology from Grade Data. In: *AusIMM Monograph 30: Mineral Resource and Ore Reserve Estimation — The AusIMM Monograph, Guide to Good Practice*, 30, Melbourne, p. 207-220.

Cox S.F. 2005. Coupling between deformation, fluid pressures, and fluid flow in ore-producing hydrothermal systems at depth in the crust. *Economic Geology*, **100**:39-75. https://doi.org/10.5382/AV100.04

Cunha I.A., Coelho C.E.S., Misi A. 2000. Fluid inclusion study of the Morro Agudo Pb–Zn deposit, Minas Gerais, Brazil. *Revista Brasileira de Geociências*, **30**:318-321. https://doi.org/10.25249/0375-7536.2000302318321

Cunha I.A., Misi A., Babinski M. 2007. Lead isotope constraints on the genesis of Pb–Zn deposits of the Neoproterozoic Vazante Group, Minas Gerais, Brazil. *Gondwana Research*, **11**(3):382-395. https://doi.org/10.1016/j.gr.2006.02.008

Dardenne M.A. 1974. Geologia da região de Vazante, Minas Gerais, Brasil. 25º Congresso Brasileiro de Geologia, Porto Alegre. *Resumos*, p. 182-185.

Dardenne M.A. 2000. The Brasília Fold Belt. In: Cordani U.G., Milani E.J., Thomaz Filho A., Campos D.A. (eds.). *The Tectonic Evolution of South America*. 31st International Geological Congress. Rio de Janeiro, p. 231-263.

Dardenne M.A. 2001. Lithostratigraphic sedimentary sequences of the Vazante Group. In: Misi A., Teixeira J.B.G. (eds.). 1st IGCP 450 Workshop, Proterozoic Sediment-Hosted Base Metal Deposits of Western Gondwana, Belo Horizonte. *Abstracts*, p. 48-50.

Dardenne M.A., Freitas-Silva F.H. 1999. Pb–Zn ore deposits of Bambuí and Vazante Groups in the São Francisco Craton and Brasilia Fold Belt, Brazil. In: Silva M.G., Misi A. (Eds.), *Base Metal Deposits of Brazil*. Salvador: MME-Brazil, p. 75-83.

Dardenne M.A., Freitas-Silva F.H., Souza J.C.F., Campos J.E.G. 1998. Evolução tectono-sedimentar do Grupo Vazante no contexto da Faixa de Dobramentos Brasília. *40º Congresso Brasileiro de Geologia*, Belo Horizonte. *Anais*, p. 26.

Freitas-Silva F.H. 1991. *Enquadramento lito-estratigráfico e estrutural do depósito de ouro de Morro do Ouro, Paracatu/MG*. MS Dissertation, Instituto de Geociências, Universidade de Brasília, Brasília, 151 p.

Geboy N.J., Kaufman A.J., Walker R.J., Misi A., Oliveira T.F., Miller K.E., Azmy K., Kendall B., Pouton S.W. 2013. Re–Os age constraints and new observations of glacial deposits in the Mesoproterozoic Vazante Group Brazil. *Precambrian Research*, **238**:199-213. https://doi.org/10.1016/j.precamres.2013.10.010

Ghazban F., McNutt R.H., Schwarcz H.P. 1994. Genesis of sediment-hosted Zn-Pb-Ba deposits in the Irankuh District, Esfahan area, west-central Iran. *Economic Geology*, **89**(6):1262-1278. https://doi.org/10.2113/gsecongeo.89.6.1262

Hardman R.F.P., Booth J.E. 1991. The significance of normal faults in the exploration and production of hydrocarbons. In: Roberts A.M., Yielding G., Freeman B. (eds.). *The Geometry of Normal Faults*, 56. London: Geological Society, p. 1-13.

Hou Z., Zhang H. 2015. Geodynamics and metallogeny of the eastern Tethyan metallogenic domain. *Ore Geology Reviews*, **70**:346-384. https://doi.org/10.1016/j.oregeorev.2014.10.026

Lanari P., Vho A., Bovay T., Airaghi L., Centrella S. 2019. Quantitative compositional mapping of mineral phases by electron probe micro-analyser. *Geological Society of London Special Publications*, **478**:39-63. https://doi.org/10.1144/SP478.4

Lanari P., Vidal O., Andrade V., Dubacq B., Lewin E., Grosch E.G., Schwartz S. 2014. XMapTools: A MATLAB©-based program for electron microprobe X-ray image processing and geothermobarometry. *Computers & Geosciences*, **62**:227-240. https://doi.org/10.1016/j.cageo.2013.08.010

Leach D.L., Bradley D.C., Huston D., Pisarevsky S.A., Taylor R.D., Gardoll, S.J. 2010. Sediment-hosted lead-zinc deposits in Earth history. *Economic Geology*, **105**(3):593-625. https://doi.org/10.2113/gsecongeo.105.3.593

Liaghat S., Moore F., Jami M. 2000. The Kuh-e-Surmeh mineralization, a carbonate-hosted Zn-Pb deposit in the Simply Folded Belt of the Zagros Mountains, SW Iran. *Mineralium Deposita*, **35**(1):72-78. https://doi.org/10.1007/s001260050007

Marcia L. 2014. *Studio Geologico Strutturale del Settore della Faixa Brasiliana compreso tra Paracatu e Vazante (Minas Gerais - Brasile)*. MS Dissertation, Facolta di Scienze, Universita' degli Studi di Cagliari, Cagliari, 93 p.

Marjoribanks R. 2010. Appendix B: Oriented Drill Core: Techniques and Procedures. In: Marjoribanks R. *Geological Methods in Mineral Exploration and Mining*. 2ª ed. Springer Science & Business Media, p. 183-204.

Martins-Neto M.A. 2009. Sequence stratigraphic framework of Proterozoic successions in eastern Brazil. *Marine and Petroleum Geology*, **26**(2):163-176. https://doi.org/10.1016/j.marpetgeo.2007.10.001

McKinstry H.E. 1948. *Mining Geology*. Englewood Cliffs: Prentice-Hall, 680 p.

Milani E.J., Davison I. 1988. Basement control and transfer tectonics in the Recôncavo-Tucano-Jatobá rift, Northeast Brazil. *Tectonophysics*, **154**(1-2):41-70. https://doi.org/10.1016/0040-1951(88)90227-2

Misi A., Azmy K., Kaufman A.J., Oliveira T.F., Sanches A.L., Oliveira G.D. 2014. Review of the geological and geochronological framework of the Vazante sequence, Minas Gerais, Brazil: Implications to metallogenic and phosphogenic models. *Ore Geology Reviews*, **63**:76-90. https://doi.org/10.1016/j.oregeorev.2014.05.002

Misi A., Iyer S.S., Coelho C.E.S., Tassinari C.C.G., Franca-Rocha W.J.S., Cunha I.D., Gomes A.S.R., Oliveira T.F., Teixeira J.B.G., Filho V.M.C. 2005. Sediment-hosted lead–zinc deposits of the Neoproterozoic Bambui Group and correlative sequences, Sao Francisco craton, Brazil: a review and a possible metallogenic evolution model. *Ore Geology Reviews*, **26**(3-4):263-304. https://doi.org/10.1016/j.oregeorev.2004.12.004

Misi A., Iyer S.S., Kyle J.R., Coelho C.E.S., Franca-Rocha W.J.S., Gomes A.S.R., Cunha I.A., Carvalho I.G. 1999. Geological and isotopic constraints on the metallogenic evolution of the Proterozoic sediment-hosted Pb–Zn (Ag) deposits of Brazil. *Gondwana Research*, **2**(1):47-65. https://doi.org/10.1016/S1342-937X(05)70126-X

Monteiro L.V.S. 2002. *Modelamento metalogenético dos depósitos de zinco de Vazante, Fagundes e Ambrósia, associados ao Grupo Vazante, Minas Gerais*. PhD Thesis, Instituto de Geociências, Universidade de São Paulo, São Paulo, 317 p.

Monteiro L.V.S., Bettencourt J.S., Juliani C., Oliveira T.F. 2006. Geology, petrography, and mineral chemistry of the Vazante non-sulfide and Ambrósia and Fagundes sulfide-rich carbonate-hosted Zn-(Pb) deposits, Minas Gerais, Brazil. *Ore Geology Reviews*, **28**(2):201-234. https://doi.org/10.1016/j.oregeorev.2005.03.005

Monteiro L.V.S., Bettencourt J.S., Juliani C., Oliveira T.F. 2007. Nonsulfide and sulfide-rich zinc mineralizations in the Vazante, Ambrósia and Fagundes deposits, MG, Brazil: mass balance and stable isotope constraints on the hydrothermal alterations. *Gondwana Research*, **11**(3):362-381. https://doi.org/10.1016/j.gr.2006.04.017

Monteiro L.V.S., Bettencourt J.S., Spiro B., Graca R., Oliveira, T.F. 1999. The Vazante zinc mine, Minas Gerais, Brazil; constraints in willemitic mineralization and fluid evolution. *Exploration and Mining Geology*, **8**(1-2):21-42.

Newhouse W.H. 1942. *Ore Deposits as Related to Structural Features*. Princeton: Princeton University Press, 280 p.

Pedrosa-Soares A.C., Noce C.M., Alkmim F.F., Silva L.C., Babinski M., Cordani U.G., Castaneda C. 2007. Orógeno Araçuaí: síntese do conhecimento 30 anos após Almeida 1977. *Geonomos*, **15**(1):1-16. https://doi.org/10.18285/geonomos.v15i1.103

Pedrosa-Soares A.C., Noce C.M., Wiedemann C.M., Pinto C.P. 2001. The Araçuaí-West-Congo orogen in Brazil: an overview of a confined orogen formed during Gondwanaland assembly. *Precambrian Research*, **110**(1-4):307-323. https://doi.org/10.1016/S0301-9268(01)00174-7

Pereira L., Dardenne M.A., Rosière C.A., Pedrosa-Soares A.C. 1994. Evolução Geológica dos Grupos Canastra e Ibiá na região entre Coromandel e Guarda-Mor, MG. *Revista Geonomos*, **2**(1):22-32. https://doi.org/10.18285/geonomos.v2i1.229

Pimentel M.M. 2016. The tectonic evolution of the Neoproterozoic Brasília Belt, central Brazil: a geochronological and isotopic approach. *Brazilian Journal of Geology*, **46**(Suppl. 1):67-82. https://doi.org/10.1590/2317-4889201620150004

Pimentel M.M., Dardenne M.A., Fuck R.A., Viana M.G., Junges S.L., Fischel D.P., Seer H.J., Dantas E.L. 2001. Nd isotopes and the provenance of detrital sediments of the Neoproterozoic Brasília Belt, central Brazil. *Journal of South American Earth Sciences*, **14**(6):571-585. https://doi.org/10.1016/S0895-9811(01)00041-4

Pimentel M.M., Fuck R.A. 1992. Neoproterozoic crustal accretion in central Brazil. *Geology*, **20**(4):375-379. https://doi.org/10.1130/0091-7613(1992)020%3C0375:NCAICB%3E2.3.CO;2

Pimentel M.M., Rodrigues J.B., DellaGiustina M.E.S., Junges S.L., Matteini M. 2011. The Tectonic Evolution of the Neoproterozoic Brasília Belt, Central Brazil, based on SHRIMP and LA-ICPMS U-Pb sedimentary provenance data: a review. *Journal of South America Earth Sciences*, **31**(4):345-357. https://doi.org/10.1016/j.jsames.2011.02.011

Pinho J.M.M. 1990. *Evolução Tectônica da mineralização de zinco de Vazante*. MS Dissertation, Instituto de Geociências, Universidade de Brasília, Brasília, 115 p.

Pinho J.M.M., Dardenne M.A., Rigobello A.E. 1989. Evolução tectônica da mineralização de zinco de Vazante. 5º Simpósio de Geologia do Núcleo Minas Gerais. *Anais*, p. 275-276.

Pinho J.M.M., Dardenne M.A., Rigobello A.E. 1990. Caracterização da movimentação transcorrente da falha de Vazante, Vazante, MG. 36º Congresso Brasileiro de Geologia. *Anais*, p. 89.

Reis H.L.S., Alkmim F.F. 2015. Anatomy of a basin-controlled foreland fold-thrust belt curve: the Três Marias salient, São Francisco basin, Brazil. *Marine and Petroleum Geology*, **66**(Part 4):711-731. https://doi.org/10.1016/j.marpetgeo.2015.07.013

Reis H.L.S., Suss J.F. 2016. Mixed carbonate-siliciclastic sedimentation in forebulge grabens: an example from the Ediacaran Bambuí Group, São Francisco basin, Brazil. *Sedimentary Geology*, **339**:83-103. https://doi.org/10.1016/j.sedgeo.2016.04.004

Reis H.L.S., Suss J.F., Fonseca R.C., Alkmim F.F. 2017. Ediacaran forebulge grabens of the southern São Francisco basin, SE Brazil: Craton interior dynamics during West Gondwana assembly. *Precambrian Research*, **302**:150-170. https://doi.org/10.1016/j.precamres.2017.09.023

Rodrigues J.B., Pimentel M.M., Buhn B., Matteini M., Dardenne M.A., Alvarenga C.J.S., Armstrong R.A. 2012. Provenance of the Vazante Group: New U–Pb, Sm–Nd. Lu–Hf isotopic data and implications for the tectonic evolution of the Neoproterozoic Brasilia Belt. *Gondwana Research*, **21**(2-3):439-450. https://doi.org/10.1016/j.gr.2011.07.017

Romeiro-Silva P.C., Zalán P.V. 2007. Contribuição da sísmica de reflexão na determinação do limite oeste do Cráton do São Francisco. *Boletim de Geociências da Petrobras*, **15**:561-571.

Rostirolla S.P., Mancini F., Reis Neto J.M., Figueira E.G., Araújo E.C. 2002. Análise estrutural da mina de vazante e adjacências: geometria, cinemática e implicações para a hidrogeologia. *Revista Brasileira de Geociências*, **32**:59-68. https://doi.org/10.25249/0375-7536.20023215968

Sial A.N., Dardenne M.A., Misi A., Pedreira A., Ferreira V.P., Silva Filho M.A., Uhlein A., Pedrosa-Soares A.C., Santos R.V., Egydio-Silva M., Babinski M., Alvarenga C.J., Fairchild T.R., Pimentel M.M. 2009. The São Francisco paleocontinent. In: Gaucher C., Sial A.N., Halverson G.P., Frimmel H.E. (eds.), *Neoproterozoic-cambrian Tectonics, Global Change and Evolution:* A Focus on South Western Gondwana, Developments in Precambrian Geology. Stuttgart: Elsevier, p. 31-69.

Sibson R.H. 1996. Structural permeability of fluid-driven fault-fracture meshes. *Journal of Structural Geology*, **18**(8):1031-1042. https://doi.org/10.1016/0191-8141(96)00032-6

Sibson R.H. 2000. Fluid involvement in normal faulting. *Journal of Geodynamics*, **29**(3-5):469-499. https://doi.org/10.1016/S0264-3707(99)00042-3

Sibson R.H., Robert F., Poulsen K.H. 1988. High-angle reverse faults, fluid-pressure cycling, and mesothermal gold-quartz deposits. *Geology*, **16**(6):551-555. https://doi.org/10.1130/0091-7613(1988)016%3C0551:HARFFP%3E2.3.CO;2

Valeriano C.M., Dardenne M.A., Fonseca M.A., Simões L.S.A., Seer H.J. 2004. A evolução tectônica da Faixa Brasília. In: Mantesso-Neto V., Bartoreli A. (eds.). *Geologia do continente sul-americano: evolução da obra de Fernando Flávio Marques de Almeida*. São Paulo: Beca, p. 575-593.

Valeriano C.M., Pimentel M.M., Heilbron M., Almeida J.C.H., Trouw R.A.J. 2008. Tectonic evolution of the Brasília Belt, central Brazil, and early assembly of Gondwana. In: Pankhurst R.J., Trouw R.A.J., Brito Neves B.B., Wit M.J. (eds.). *West Gondwana: Pre-cenozoic correlations across the South Atlantic region.* London: Geological Society, p. 197-210.

Zhang H., Yang T., Hou Z., Song Y, Liu Y, Yang Z., Tian S. 2017. Structural controls on carbonate-hosted Pb–Zn mineralization in the Dongmozhazhua deposit, central Tibet. *Ore Geology Reviews*, **90**:863-876. https://doi.org/10.1016/j.oregeorev.2017.02.008

Zimmer P.W. 1963. Orientation of small diameter core. *Economic Geology*, **58**(8):1313-1325. https://doi.org/10.2113/gsecongeo.58.8.1313